

The built-in selection bias of hazard ratios formalized

Richard A.J. Post · Edwin R. van den Heuvel · Hein Putter

Received: date / Accepted: date

Abstract It is known that the hazard ratio lacks a useful causal interpretation. Even for data from a randomized controlled trial, the hazard ratio suffers from built-in selection bias as, over time, the individuals at risk in the exposed and unexposed are no longer exchangeable. In this work, we formalize how the observed hazard ratio evolves and deviates from the causal hazard ratio of interest in the presence of heterogeneity of the hazard of unexposed individuals (frailty) and heterogeneity in effect (individual modification). For the case of effect heterogeneity, we define the causal hazard ratio. We show that the observed hazard ratio equals the ratio of expectations of the latent variables (frailty and modifier) conditionally on survival in the world with and without exposure, respectively. Examples with gamma, inverse Gaussian and compound Poisson distributed frailty, and categorical (harming, beneficial or neutral) effect modifiers are presented for illustration. This set of examples shows that an observed hazard ratio with a particular value can arise for all values of the causal hazard ratio. Therefore, the hazard ratio can not be used as a measure of the causal effect without making untestable assumptions, stressing the importance of using more appropriate estimands such as contrasts of the survival probabilities.

Keywords Causal inference · Causal hazard ratio · Selection bias · Individual effect modification · Heterogeneity of treatment effects

Mathematics Subject Classification (2020) 62D20, 62N02

R.A.J. Post
Department of Mathematics and Computer Science, Eindhoven University of Technology, The Netherlands
E-mail: r.a.j.post@tue.nl

E.R. van den Heuvel
Department of Mathematics and Computer Science, Eindhoven University of Technology, The Netherlands

H. Putter
Department of Biomedical Data Sciences, Leiden University Medical Center, The Netherlands

1 Introduction

When interested in time-to-event outcomes, ideally, one would like to know the hazard rates of an individual in the worlds with and without exposure. In practice, the focus is on the ratio of the expected hazard rates in both worlds. It is then standard practice to fit the observed hazard rates with a (time-invariant) Cox model (Cox, 1972). A decade ago, Hernán (2010) raised awareness that hazard ratios estimated from a randomized controlled trial (RCT) are not suited for causal inference. Firstly, the average hazard ratio could be uninformative as there will typically be time-varying period-specific hazard ratios. More importantly, even if period-specific hazard ratios are estimated, these can vary solely due to the loss of randomization over time by conditioning on survivors. The exposure assignment and risk factors become dependent when conditioning on individuals that survived t , i.e. survival time $T \geq t$, even if these risk factors are unrelated to the exposure (Aalen et al., 2015). As a result, effect measures based on hazards can suffer from non-collapsibility (Daniel et al., 2021; Sjölander et al., 2016; Aalen et al., 2015; Martinussen and Vansteelandt, 2013).

In practice, the wrong estimand, a ratio of (partly) marginalized hazards, is defined, that by the non-collapsibility, deviates from the conditional (causal) hazard ratio. This contrast is referred to as the built-in selection bias of hazard ratios as the non-collapsibility results from conditioning on prior survival (Hernán, 2010; Aalen et al., 2015; Sjölander et al., 2016; Stensrud et al., 2018; Young et al., 2020; Martinussen et al., 2020). This bias should not be confused with confounding bias that is absent when using data from an RCT (Didelez and Stensrud, 2021). For exposure assignment A , and the potential survival time when the exposure is intervened on to a denoted by T^a , the observed hazard ratio from an RCT satisfies

$$\frac{\lim_{h \rightarrow 0} h^{-1} \mathbb{P}(T \in [t, t+h) \mid T \geq t, A = a)}{\lim_{h \rightarrow 0} h^{-1} \mathbb{P}(T \in [t, t+h) \mid T \geq t, A = 0)} = \frac{\lim_{h \rightarrow 0} h^{-1} \mathbb{P}(T^a \in [t, t+h) \mid T^a \geq t)}{\lim_{h \rightarrow 0} h^{-1} \mathbb{P}(T^0 \in [t, t+h) \mid T^0 \geq t)} \quad (1)$$

(De Neve and Gerds, 2020; Martinussen et al., 2020). The observed hazard ratio thus equals the ratio of hazard rates at time t for the potential outcomes of individuals from different populations; those for which $T^a \geq t$ and those for which $T^0 \geq t$. As already indicated before, these populations will typically not be exchangeable in other risk factors, implying that an effect found cannot be (solely) assigned to the exposure. The effect does thus not reflect how the hazard rate of an individual is affected by exposure. Only for cause-effect relations such that (1) is time-invariant, the estimand can be interpreted as

$$\frac{\log(\mathbb{P}(T^a \geq t))}{\log(\mathbb{P}(T^0 \geq t))}.$$

It has therefore been recommended to use better interpretable estimands such as contrasts of quantiles, the restricted mean survival or survival probabilities of the potential outcomes respectively (Hernán, 2010; Bartlett et al., 2020; Stensrud et al., 2018; Young et al., 2020), or the probabilistic index derived from the latter (De Neve and Gerds, 2020). Alternatively, one can avoid interpretation issues by using accelerated failure time models (Hernán, 2010; Hernán et al., 2005) or additive hazard models (Aalen et al., 2015; Martinussen et al., 2020).

Nevertheless, particularly in medical sciences, marginal hazard ratios are still commonly presented by practitioners. To boost the recommended paradigm shift, we would like to quantify the contrast between the causal hazard ratio and the observed hazard ratio, i.e. the built-in selection bias. To do so, we start by presenting a general parameterization of cause-effect relations for time-to-event outcomes using a structural causal model. This parameterization clearly defines the causal effect of an exposure on an individual's hazard and, as such, allows us to define the causal hazard ratio. The quantitative examples in which the hazard under no exposure varies among individuals, i.e. frailty, as presented in the literature (Stensrud et al., 2017;

Aalen et al., 2015; Balan and Putter, 2020) do fit in our framework, and we will formalize results for these examples. Additionally, we will extend these examples with causal effect heterogeneity, i.e. the causal effect on the hazard rate might vary between individuals (Stensrud et al., 2017).

2 Notation

In this work, probability distributions of factual and counterfactual outcomes are defined in terms of the potential outcome framework (Rubin, 1974; Neyman, 1990). Let T_i and A_i represent the (factual) stochastic outcome and exposure assignment level of individual i . Let T_i^a equal the potential outcome of individual i under an intervention of level a (counterfactual when $A_i \neq a$). For those more familiar with the do-calculus, T^a is equivalent to $T \mid do(A = a)$ as e.g. derived in Pearl (2009, Equation 40) and Bongers et al. (2021, Definition 8.6). Throughout this work, we will assume causal consistency: if $A_i = a$, then $T_i^a = T_i^{A_i} = T_i$, implying that potential outcomes are independent of the exposure levels of other individuals (no interference).

The hazard rate of T^a can vary among the individuals in the population of interest. We will parameterize this heterogeneity for hazards of T^0 using a random variable U_{0i} that represents the frailty of individual i (Balan and Putter, 2020). The absolute effect of an exposure on the hazard, i.e. the contrast between the hazard rates of T_i^0 and T_i^a respectively, can depend on U_{0i} . However, there might also be (relative) effect heterogeneity that we parameterize using the random variable U_{1i} , giving rise to an individual-specific hazard ratio. The hazard of the potential outcome T_i^a can be parameterized with a function that depends on U_{0i} , U_{1i} and a . We focus on cause-effect relations that can be parameterized with a structural causal model (SCM)¹, that consists of a joint probability distribution of (N_A, U_0, U_1, N_T) and a collection of structural assignments (f_A, f_λ) such that

$$\begin{aligned} A_i &:= f_A(N_{Ai}) \\ \lambda_i^a(t) &:= f_\lambda(t, U_{0i}, U_{1i}, a) \\ T_i^a &:= \min\{t > 0 : e^{-\Lambda_i^a(t)} \leq N_{Ti}\}, \end{aligned} \tag{2}$$

where $\Lambda_i^a(t) = \int_0^t \lambda_i^a(s) ds$, $f_\lambda(t, U_{0i}, U_{1i}, 0) \perp\!\!\!\perp U_{1i}$, i.e. when $a = 0$ f_λ does not contain U_1 , and $N_{Ai}, N_{Ti} \sim \text{Uni}[0, 1]$, while $U_{0i}, U_{1i} \perp\!\!\!\perp N_{Ti}$ and f_A is the inverse cumulative distribution function of A .

Note that the data generating mechanism is described by this SCM as $T_i^{A_i} = T_i$. For the distribution of data observed from an RCT, we have that $N_A \perp\!\!\!\perp U_0, U_1, N_T$, i.e. no confounding, as a result of the randomization. Note that $\lambda_i^a(t)$ equals the hazard of the potential outcome of individual i under exposure a , i.e. $\lambda_i^a(t) = \lim_{h \rightarrow 0} h^{-1} \mathbb{P}(T_i^a \in [t, t+h] \mid T_i^a \geq t, U_{0i}, U_{1i})$. In this parameterization, U_0 thus results in heterogeneity of the hazard under no exposure between individuals, and the presence of U_1 results in heterogeneity of the effect of the exposure on the hazard between individuals. The SCM could be re-parameterized by including more details, e.g. measured risk factors, so that the remaining (conditional) unmeasured heterogeneity will be less variable.

Formulation of hazard rates of potential outcomes presented in the literature, e.g. by Aalen et al. (2015) and by Stensrud et al. (2017), naturally fit in this parameterization. However, the dependence of T^a and

¹ A structural causal model as presented in this work is a union of the traditional SCM, for $a = A$, and the intervened SCMs for all possible $do(A = a)$ as e.g. presented in Peters et al. (2018).

T^0 beyond shared frailty is typically not specified. The causal relations in SCM (2) can be visualized in a graph. In Figure 1, one can observe this so-called Single-World Intervention Graph (SWIG) as proposed by Richardson and Robins (2013) unified with the traditional causal directed acyclic graph (DAG) (Pearl, 2009).

It is insightful to realize that T_i^a depends on a and the random variables U_{0i} , U_{1i} , N_{Ti} only, i.e.

$$T_i^a := \min\{t > 0 : e^{-\int_0^t f_\lambda(U_{0i}, s, U_{1i}, a) ds} \leq N_{Ti}\} = g(U_{0i}, U_{1i}, N_{Ti}, a),$$

for some function g , so by randomization

$$T_i^a \perp\!\!\!\perp A_i. \quad (3)$$

However, it should be noted that

$$T_i^a \not\perp\!\!\!\perp A_i \mid T_i \geq t, \quad (4)$$

as $T_i := g(U_{0i}, U_{1i}, N_{Ti}, A_i)$, so that $A_i \mid T_i \geq t$ does inform on (U_{0i}, U_{1i}, N_{Ti}) and thus on T_i^a . In the literature, (4) is often implicitly derived by recognizing that $\{T \geq t\}$ is a collider in Figure 1, and thus opens a back-door path between A and T^a (Aalen et al., 2015; Sjölander et al., 2016). The bias that results from conditioning on this collider is often referred to as the built-in selection bias of the hazard ratio. More general, in causal inference, selection bias is caused by conditioning on a variable G that induces dependence between Y^a and A , i.e. $Y^a \perp\!\!\!\perp A$ but $Y^a \not\perp\!\!\!\perp A \mid G$, see e.g. Hernán and Robins (2020, Chapter 8). By causal consistency $Y^a \mid \{G, A = a\} \stackrel{d}{=} Y \mid G, A = a$ but $Y^a \mid G \stackrel{d}{\neq} Y^a \mid \{G, A = a\}$, so $Y^a \mid G \stackrel{d}{\neq} Y \mid G, A = a$ (as is the case in Equation (4) for $G = \{T \geq t\}$). However, the built-in selection bias is subtle as the dependence is a consequence of conditioning a potential outcome on information on its factual outcome, while it should be noted that (for an RCT),

$$T_i^a \perp\!\!\!\perp A_i \mid T_i^a \geq t, \quad (5)$$

again as $T_i^a := g(U_{0i}, U_{1i}, N_{Ti}, a)$, $A_i \mid T_i^a \geq t$ does not inform on (U_{0i}, U_{1i}, N_{Ti}) . A more standard example of selection bias for survival analysis from an RCT is not accounting for informative censoring ($C = 1$) (Hernán et al., 2004; Howe et al., 2016), in which case

$$T^a \mid \{C = 0\} \stackrel{d}{\neq} T^a \mid \{C = 0, A = a\}.$$

When interested in the causal effect, we should try to express the distribution of potential outcomes in terms of the observed distribution as we will do in the next section.

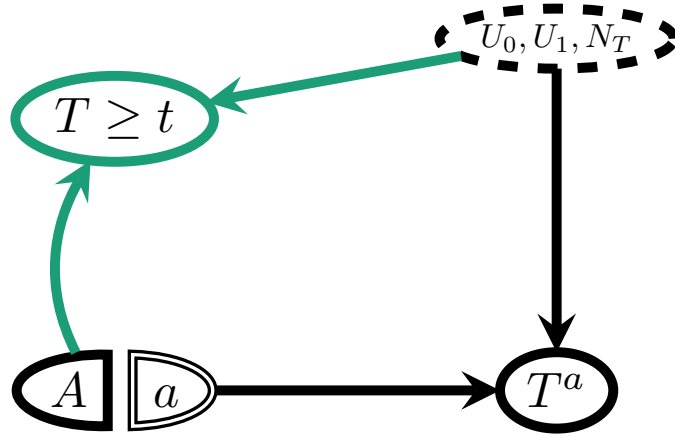


Fig. 1: The SWIG (black) extended with the DAG (green) for SCM (2), visualizing the causal relations between the exposure assignment A , the observed survival indicator $\{T \geq t\}$ and the potential survival time T^a .

3 The causal hazard ratio

Parameterization of the cause-effect relations with SCM (2) allows us to define the causal hazard ratio. If

$$f_\lambda(t, U_{0i}, U_{1i}, a) = f_0(t, U_{0i})f_1(t, U_{1i}, a) \text{ and } f_1(t, U_{1i}, 0) = 1,$$

then the individual causal effect is captured by $f_1(t, U_{1i}, a)$. The latter equals the ratio of the hazard of an individual's potential outcome when exposed and when non-exposed at time t , i.e. $\frac{\lambda_i^a(t)}{\lambda_i^0(t)}$. In the case of homogeneous effects, $f_1(t, U_{1i}, a) = f_1(t, a)$ is equal for all individuals and would thus be the estimand of interest. In the case of heterogeneity of effects, $f_1(t, U_{1i}, a)$ is the individual multiplicative causal effect. From a public health perspective, the ratio of the expected hazard in the world where everyone is exposed to a and the expected hazard in the world where all individuals are unexposed is of interest. This causal hazard ratio (CHR) of interest can be obtained as the ratio of the marginalized (over U_0 and U_1) conditional hazard rates in both worlds as presented in Definition 1.

Definition 1 Causal hazard ratio The causal hazard ratio (CHR) for cause-effect relations that can be parameterized with SCM 2 equals

$$\begin{aligned} \frac{\mathbb{E}[\lambda_i^a(t)]}{\mathbb{E}[\lambda_i^0(t)]} &= \frac{\mathbb{E}[\lim_{h \rightarrow 0} h^{-1} \mathbb{P}(T^a \in [t, t+h) \mid T^a \geq t, U_0, U_1)]}{\mathbb{E}[\lim_{h \rightarrow 0} h^{-1} \mathbb{P}(T^0 \in [t, t+h) \mid T^0 \geq t, U_0)]} \\ &= \frac{\int \lim_{h \rightarrow 0} h^{-1} \mathbb{P}(T^a \in [t, t+h) \mid T^a \geq t, U_0, U_1) dF_{U_0, U_1}}{\int \lim_{h \rightarrow 0} h^{-1} \mathbb{P}(T^0 \in [t, t+h) \mid T^0 \geq t, U_0) dF_{U_0}}, \end{aligned} \quad (6)$$

where we abbreviate the Lebesgue-Stieltjes integral of a function g with respect to probability law F_X , i.e. $\int g(x) dF_X(x)$, as $\int g(X) dF_X$.

Note that, when $U_0 \not\perp U_1$, the CHR can differ from the expectation of an individual's multiplicative effect ($\mathbb{E}[\frac{\lambda_i^a(t)}{\lambda_i^0(t)}]$). For cause-effect relations of a binary exposure that can be parameterized with SCM (2) such

that $f_\lambda(t, U_{0i}, U_{1i}, a) = U_{0i}\lambda_0(t)(U_{1i})^a$ and $\mathbb{E}[U_0] = 1$, $\frac{\mathbb{E}[\lambda_i^1(t)]}{\mathbb{E}[\lambda_i^0(t)]} = \mathbb{E}[U_0U_1] = \mathbb{E}[U_1] + \text{cov}(U_0, U_1)$ while $\mathbb{E}\left[\frac{\lambda_i^1(t)}{\lambda_i^0(t)}\right] = \mathbb{E}[U_1]$.²

When the parameterization of the cause-effect relations as SCM (2) would be known, the CHR can be expressed in terms of the distribution of the data generating mechanism as presented in Theorem 1.

Theorem 1 *If the cause-effect relations of interest can be parameterized with SCM (2), and $N_A \perp U_0, U_1, N_T$ (no confounding) then*

$$\frac{\mathbb{E}[\lambda_i^a(t)]}{\mathbb{E}[\lambda_i^0(t)]} = \frac{\int \lim_{h \rightarrow 0} h^{-1} \mathbb{P}(T \in [t, t+h] \mid T \geq t, U_0, U_1, A = a) dF_{U_0, U_1}}{\int \lim_{h \rightarrow 0} h^{-1} \mathbb{P}(T \in [t, t+h] \mid T \geq t, U_0, A = 0) dF_{U_0}}.$$

Consider, for example, the commonly used frailty model where effect heterogeneity is absent, i.e.

$$\lambda_i^a(t) = U_{0i}\lambda_0(t)f_1(t, a).$$

The CHR equals the multiplicative effect that does not differ among individuals and equals $f_1(t, a)$. By applying Theorem 1, this CHR is indeed derived to equal

$$\frac{\int \lim_{h \rightarrow 0} h^{-1} \mathbb{P}(T \in [t, t+h] \mid T \geq t, U_0, A = a) dF_{U_0}}{\int \lim_{h \rightarrow 0} h^{-1} \mathbb{P}(T \in [t, t+h] \mid T \geq t, U_0, A = 0) dF_{U_0}} = \frac{f_1(t, a)\lambda_0(t)\mathbb{E}[U_0]}{\lambda_0(t)\mathbb{E}[U_0]} = f_1(t, a). \quad (7)$$

It is important to note that (7) deviates from the observed hazard ratio equal to

$$\frac{\lim_{h \rightarrow 0} h^{-1} \mathbb{P}(T \in [t, t+h] \mid T \geq t, A = a)}{\lim_{h \rightarrow 0} h^{-1} \mathbb{P}(T \in [t, t+h] \mid T \geq t, A = 0)} = \frac{f_1(t, a)\lambda_0(t)\mathbb{E}[U_0 \mid T \geq t, A = a]}{\lambda_0(t)\mathbb{E}[U_0 \mid T \geq t, A = 0]},$$

as we will elaborate on in Section 4.

In summary, it becomes clear that to derive the CHR from data, inference on the distribution of the latent frailty U_0 and effect modifier U_1 must be made. When their distributions are known, inference can be drawn from observed data, even when the parameters of the distributions are unknown. Software available to estimate frailty parameters are described by Balan and Putter (2020), and such methods could also be adapted to estimate the latent modifier distribution. However, in practice, the distributions of these latent variables are unknown. Even in the case without causal effect heterogeneity, it is impossible to distinguish the presence of frailty from a time-dependent causal effect (Balan and Putter, 2020, Section 2.5). More precisely, different combinations of (varying) effect sizes and frailty distributions give rise to the same marginal distribution. The same holds for combinations that also involve effect modifiers. In the case of clustered survival data, at least theoretically, the shared frailty could be distinguished from violation of proportional hazards (Balan and Putter, 2020). Reasoning along the same lines, individual frailty and marginal time-varying effects could only be derived from effect heterogeneity in the case of recurrent events with stationary distributions.

² Consider for example,

$$(U_0, U_1) = \begin{cases} (0.5, 1.5) & p = 0.5 \\ (1.5, 0.5) & p = 0.5, \end{cases}$$

so that apart from $\mathbb{E}[U_0] = 1$ also $\mathbb{E}[U_1] = 1$ and $U_0U_1 = \frac{3}{4}$ for everyone. As a result of the exposure, the hazard of 50% of the individuals would increase by 50% ($0.5\lambda_0(t) \rightarrow 0.75\lambda_0(t)$) and the hazard of the other 50% would decrease by 50% ($1.5\lambda_0(t) \rightarrow 0.75\lambda_0(t)$). The expected hazard rate in the world without exposure equals $\lambda_0(t)$ while the (expected) hazard in the world with exposure equals $0.75\lambda_0(t)$. On average, living in a world with exposure is thus more beneficial.

4 Marginal causal hazard ratio

In Theorem 1, the actual CHR (see Definition 1) has been expressed in terms of the distribution of the observed data, and we concluded that these are typically not identifiable. Practitioners often compute the hazard ratio from data, which expectation is referred to as the observed hazard ratio (OHR) and, in the absence of informative censoring, equals

$$\text{OHR}(t) = \frac{\lim_{h \rightarrow 0} h^{-1} \mathbb{P}(T \in [t, t+h] \mid T \geq t, A = a)}{\lim_{h \rightarrow 0} h^{-1} \mathbb{P}(T \in [t, t+h] \mid T \geq t, A = 0)}. \quad (8)$$

To compare the OHR to the CHR that quantifies the causal effect of interest, the OHR should be expressed in terms of potential outcomes. For data from an RCT, by independence (5) and causal consistency, the OHR equals the marginal causal hazard ratio (MCHR), i.e.

$$\text{MCHR}(t) = \frac{\lim_{h \rightarrow 0} h^{-1} \mathbb{P}(T^a \in [t, t+h] \mid T^a \geq t)}{\lim_{h \rightarrow 0} h^{-1} \mathbb{P}(T^0 \in [t, t+h] \mid T^0 \geq t)}. \quad (9)$$

This MCHR should not be confused with the ‘marginal causal hazard ratio’ defined by Martinussen et al. (2020) that equals

$$\frac{\lim_{h \rightarrow 0} h^{-1} \mathbb{P}(T^a \in [t, t+h] \mid T^a \geq t, T^0 \geq t)}{\lim_{h \rightarrow 0} h^{-1} \mathbb{P}(T^0 \in [t, t+h] \mid T^0 \geq t, T^a \geq t)}, \quad (10)$$

and is not considered in this work.

We will study how the MCHR (and thus the OHR from an RCT) differs from the CHR over time. By the law of total probability, (9) equals

$$\frac{\int \lim_{h \rightarrow 0} h^{-1} \mathbb{P}(T^a \in [t, t+h] \mid T^a \geq t, U_0, U_1) dF_{U_0, U_1 \mid T^a \geq t}}{\int \lim_{h \rightarrow 0} h^{-1} \mathbb{P}(T^0 \in [t, t+h] \mid T^0 \geq t, U_0) dF_{U_0 \mid T^0 \geq t}}. \quad (11)$$

As the integration in the result of Theorem 1 is with respect to the distribution of U_0 and U_1 , in the entire population, instead of those individuals for which $T^a \geq t$ or $T^0 \geq t$, the MCHR deviates from the CHR, i.e. the built-in selection bias of the hazard (Hernán, 2010; Aalen et al., 2015; Stensrud et al., 2018).

The problem induced for estimation of the CHR thus results from inference on the wrong estimand; the combined effect of the exposure of interest and the difference in latent frailty (and effect modification) distribution, is computed. This section will formalize how (9) deviates from the CHR. Let us again focus on cause-effect relations that can be parameterized with SCM (2) in which

$$\lambda_i^a(t) = f_0(t, U_{0i}) f_1(t, U_{1i}, a),$$

where the CHR equals $\mathbb{E}[f_1(t, U_1, a)]$. These would be the cause-effect relations for which the CHR is an appropriate causal effect measure. Moreover, we focus on hazard functions that satisfy Condition 1 and do thus not have an infinite discontinuity.

Condition 1 Hazard without infinite discontinuity

$$\exists \tilde{h} > 0 \text{ so that } \forall h^* \in (0, \tilde{h}) : \mathbb{E}[f_0(t+h^*, U_0) f_1(t+h^*, U_1, a) \mid T^a \geq t] < \infty$$

The real value of the MCHR, that deviates from the CHR, is derived in Theorem 2.

Theorem 2 *If the cause-effect relations of interest can be parameterized with SCM (2), where*

$$\lambda_i^a(t) = f_0(t, U_{0i})f_1(t, U_{1i}, a),$$

and Condition 1 holds, then

$$\frac{\lim_{h \rightarrow 0} h^{-1} \mathbb{P}(T^a \in [t, t+h) \mid T^a \geq t)}{\lim_{h \rightarrow 0} h^{-1} \mathbb{P}(T^0 \in [t, t+h) \mid T^0 \geq t)} = \frac{\mathbb{E}[f_0(t, U_0)f_1(t, U_1, a) \mid T^a \geq t]}{\mathbb{E}[f_0(t, U_0) \mid T^0 \geq t]} =$$

$$\int f_0(t, U_0)f_1(t, U_1, a) \frac{\exp(-\Lambda^a(t, U_0, U_1))}{\int \exp(-\Lambda^a(t, U_0, U_1)) dF_{(U_0, U_1)}} dF_{(U_0, U_1)} \left(\int f_0(t, U_0) \frac{\exp(-\Lambda^0(t, U_0))}{\int \exp(-\Lambda^0(t, U_0)) dF_{U_0}} dF_{U_0} \right)^{-1},$$

where $\Lambda^a(t, u_0, u_1) = \int_0^t f_0(s, u_0)f_1(s, u_1, a) ds$ and thus $\Lambda^0(t, u_0) = \int_0^t f_0(s, u_0) ds$.

The conditional expectations that determine the value of the MCHR equal weighted means of $f_0(t, u_0)f_1(t, u_1, a)$ and $f_0(t, u_0)$ with weights $\frac{\mathbb{P}(T^a \geq t \mid U_0 = u_0, U_1 = u_1)}{\mathbb{P}(T^a \geq t)}$ and $\frac{\mathbb{P}(T^0 \geq t \mid U_0 = u_0)}{\mathbb{P}(T^0 \geq t)}$ respectively. To develop our understanding of the bias when the OHR (assuming no confounding) is used to estimate the CHR, we will first continue to study the bias as a result of frailty and heterogeneity separately in the next two subsections.

4.1 Causal effect homogeneity

In the case of homogeneous multiplicative causal effects on the hazard, i.e. $f_1(t, U_{1i}, a) = f_1(t, a)$, the ratio of the marginal hazard rates of individuals satisfying $T_i^a \geq t$ and of those $T_i^0 \geq t$ equals $f_1(t, a)$ multiplied by a factor that depends on the difference in frailty distributions at time t in those two populations as derived in Corollary 1.

Corollary 1 *If the cause-effect relations of interest can be parameterized with SCM (2), where*

$$\lambda_i^a(t) = f_0(t, U_{0i})f_1(t, a),$$

and condition 1 holds then

$$\frac{\lim_{h \rightarrow 0} h^{-1} \mathbb{P}(T^a \in [t, t+h) \mid T^a \geq t)}{\lim_{h \rightarrow 0} h^{-1} \mathbb{P}(T^0 \in [t, t+h) \mid T^0 \geq t)} = \frac{\mathbb{E}[f_0(t, U_0) \mid T^a \geq t]}{\mathbb{E}[f_0(t, U_0) \mid T^0 \geq t]} f_1(t, a) =$$

$$\int f_0(t, U_0) \frac{\exp(-\int_0^t f_0(s, U_0)f_1(a, s) ds)}{\int \exp(-\int_0^t f_0(s, U_0)f_1(a, s) ds) dF_{U_0}} dF_{U_0} \left(\int f_0(t, U_0) \frac{\exp(-\int_0^t f_0(s, U_0) ds)}{\int \exp(-\int_0^t f_0(s, U_0) ds) dF_{U_0}} dF_{U_0} \right)^{-1} f_1(t, a).$$

The conditional expectation $\mathbb{E}[f_0(t, U_0) \mid T^a \geq t]$ can be seen as a reweighted mean of $f_0(t, u_0)$. These weights equal $\frac{\mathbb{P}(T^a \geq t \mid U_0 = u_0)}{\mathbb{P}(T^a \geq t)}$ and over time increase for favourable values of U_0 . As a result $\mathbb{E}[f_0(t, U_0) \mid T^a \geq t]$ decreases over time. If $\Lambda^a(u_0, t) > \Lambda^0(u_0, t)$, e.g. when $\forall t : f_1(t, a) > 1$, then the weights $\frac{\mathbb{P}(T^a \geq t \mid U_0 = u_0)}{\mathbb{P}(T^a \geq t)}$ decrease more rapidly with u than the weights $\frac{\mathbb{P}(T^0 \geq t \mid U_0 = u_0)}{\mathbb{P}(T^0 \geq t)}$, leading to

$$\frac{\mathbb{E}[f_0(t, U_0) \mid T^a \geq t]}{\mathbb{E}[f_0(t, U_0) \mid T^0 \geq t]} < 1. \quad (12)$$

On the contrary, when $\Lambda^a(u_0, t) < \Lambda^0(u_0, t)$, then

$$\frac{\mathbb{E}[f_0(t, U_0) \mid T^a \geq t]}{\mathbb{E}[f_0(t, U_0) \mid T^0 \geq t]} > 1. \quad (13)$$

So in the case of effect homogeneity, at time t , the MCHR is larger than the CHR when $\Lambda^a(u_0, t) < \Lambda^0(u_0, t)$ and smaller when $\Lambda^a(u_0, t) > \Lambda^0(u_0, t)$. An example of the latter was showcased by Stensrud et al. (2017), where a model with $f_1(t, a) = 1.81^a$, $f_0(u_0, t) = u_0 \lambda_0(t)$ and compound Poisson distributed frailty U_0 could well explain the decrease of the effect of hormone replacement therapy on coronary heart disease in postmenopausal women over time as observed from an RCT by the Woman Health Initiative. Furthermore, as emphasized by Hernán (2010) based on the same case-study, even when $f_1(t, a)$ is constant over time, the (bias of the) MCHR hazard is time-varying, so that the estimates can depend on the follow-up time of a study.

For frailty models as presented by Stensrud et al. (2017) and Aalen et al. (2015), where $f_0(t, U_{0i}) = U_{0i} \lambda_0(t)$, it has already been shown by Balan and Putter (2020) that $\mathbb{E}[U_0 \mid T \geq t, A = a]$ can be expressed in terms of the Laplace transform of the frailty U_0 . Reasoning along the same lines, $\mathbb{E}[U_0 \mid T^a \geq t]$ is expressed in terms of the Laplace transform of the U_0 in Lemma 1.

Lemma 1 *If the cause-effect relations of interest can be parameterized with SCM (2), where*

$$f_\lambda(t, U_{0i}, U_{1i}, a) = U_{0i} \lambda_0(t) f_1(t, a),$$

then

$$\mathbb{E}[U_0 \mid T^a \geq t] = - \frac{\mathcal{L}'_{U_0}(\int_0^t \lambda_0(s) f_1(a, s) ds)}{\mathcal{L}_{U_0}(\int_0^t \lambda_0(s) f_1(a, s) ds)}, \quad (14)$$

where $\mathcal{L}_{U_0}(c) = \mathbb{E}[\exp(-cU_0)]$ with derivative $\mathcal{L}'_{U_0}(c)$.

As in this previous work (Balan and Putter, 2020, Figure 5), we present examples where U_0 follows a gamma, inverse Gaussian or compound Poisson distribution respectively. The parameterizations, corresponding Laplace transforms and expressions for $\mathbb{E}[U_0 \mid T^a \geq t]$ can be found in Appendix B. To illustrate the selection bias, we consider a binary exposure and let

$$\lambda_i^a(t) = U_{0i} \lambda_0(t) c^a,$$

where $\lambda_0(t) = \frac{t^2}{20}$, $U_0 \sim \Gamma(\theta_0^{-1}, \theta_0)$, $U_0 \sim \text{IG}(1, \theta_0^{-1})$ or $U_0 \sim \text{CPoi}(3\theta_0^{-1}, \frac{1}{2}, \frac{2}{3}\theta_0)$ respectively, so that $\mathbb{E}[U_0] = 1$ and $\text{var}(U_0) = \theta_0$. By applying Lemma 1, $\mathbb{E}[U_0 \mid T^1 \geq t]$ and $\mathbb{E}[U_0 \mid T^0 \geq t]$ can be derived. The MCHR then follows from Corollary 1 (conditional hazard is monotone increasing). The expressions for these quantities are presented in Table 1.

How the MCHR deviates from c over time for $c \in \{\frac{1}{3}, 3\}$, and $\theta \in \{0.5, 1, 2\}$ is visualized in Figure 2. For both $c = 3$ and $c = \frac{1}{3}$ the selection of individuals that survive time t result in a MCHR that evolves in the opposite direction of the causal effect, towards 1, \sqrt{c} and $\sqrt{c^{-1}}$ respectively. For the case of a compound Poisson frailty, the logarithm of this latter limit is even opposite to the sign of the logarithm of the CHR due to the nonsusceptible individuals. For all types of frailty, the higher the variance of U_0 , the larger the difference between the MCHR and the CHR. For comparison we have also presented the survival curves of T^1 and T^0 in Figure 10 in Appendix C for the setting where $\theta_0 = 1$. Note that for an RCT $T^a \stackrel{d}{=} T \mid A = a$ by (2) and causal consistency.

Table 1: Conditional expectations and resulting MCHR when the CHR equals c for different frailty distributions such that $\mathbb{E}[U_0] = 1$ and $\text{var}(U_0) = \theta_0$ (in absence of effect modification).

	$U_0 \sim$		
	$\Gamma(\theta_0^{-1}, \theta_0)$	$\text{IG}(1, \theta_0^{-1})$	$\text{CPoi}(3\theta_0^{-1}, \frac{1}{2}, \frac{2}{3}\theta_0)$
$\mathbb{E}[U_0 T^1 \geq t]$	$\frac{60}{60+ct^3\theta_0}$	$\sqrt{\frac{30}{30+ct^3\theta_0}}$	$90^{\frac{3}{2}}(90+ct^3\theta_0)^{-\frac{3}{2}}$
$\mathbb{E}[U_0 T^0 \geq t]$	$\frac{60}{60+t^3\theta_0}$	$\sqrt{\frac{30}{30+t^3\theta_0}}$	$90^{\frac{3}{2}}(90+t^3\theta_0)^{-\frac{3}{2}}$
$\frac{\lim_{h \rightarrow 0} h^{-1} \mathbb{P}(T^1 \in (t, t+h) T^1 \geq t)}{\lim_{h \rightarrow 0} h^{-1} \mathbb{P}(T^0 \in (t, t+h) T^0 \geq t)}$	$1 + \frac{60(c-1)}{60+ct^3\theta_0}$	$c \frac{\sqrt{30+t^3\theta_0}}{\sqrt{30+ct^3\theta_0}}$	$c \left(\frac{90+t^3\theta_0}{90+ct^3\theta_0} \right)^{\frac{3}{2}}$

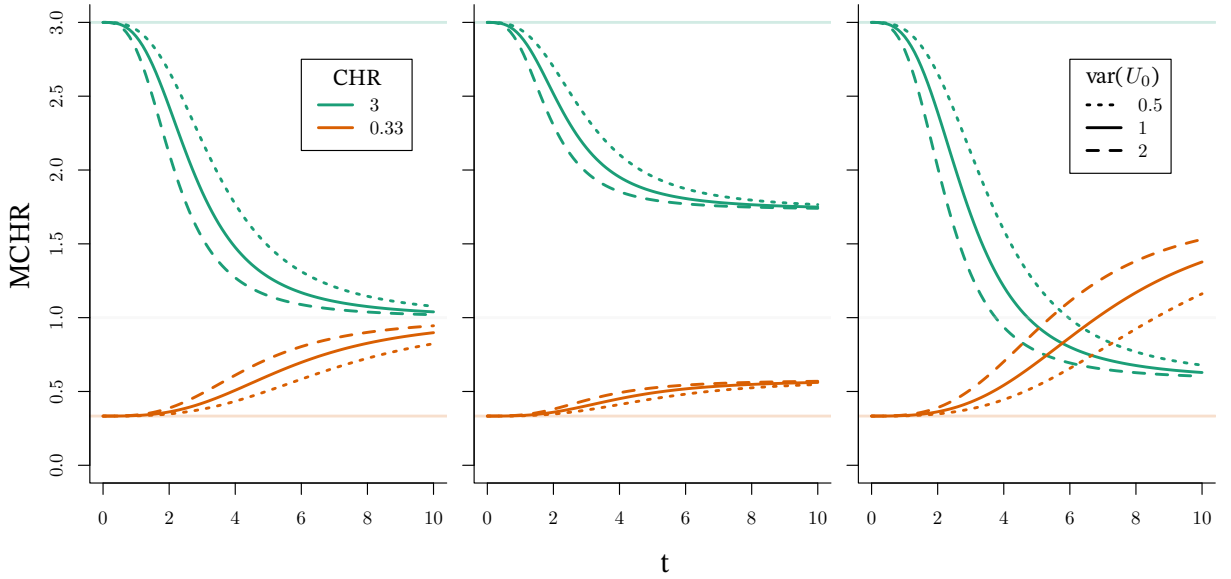


Fig. 2: MCHR over time when $\lambda_i^a(t) = U_{0i} \frac{t^2}{20} c^a$ for $c = 3$ (green) and $c = \frac{1}{3}$ (orange), when U_0 follows a gamma (left), inverse Gaussian (middle) or compound Poisson (right) distribution with variance 0.5 (dotted), 1 (solid) or 2 (dashed) respectively.

4.2 Causal effect heterogeneity in the absence of frailty

Before we return to the general case presented in Theorem 2, let's consider the presence of effect heterogeneity in the absence of frailty, i.e.

$$f_\lambda(t, U_{0i}, U_{1i}, a) = \lambda_0(t) f_1(t, U_{1i}, a).$$

If the CHR, $\mathbb{E}[f_1(t, U_{1i}, a)]$, is equal for all t , the MCHR is not as over time among the exposed individuals those that 'benefit' more are more likely to survive. The effect of this selection on the MCHR over time is formalized in Corollary 2.

Corollary 2 *If the cause-effect relations of interest can be parameterized with SCM (2), where*

$$\lambda_i^a(t) = \lambda_0(t)f_1(t, U_{1i}, a),$$

and Condition 1 holds then

$$\begin{aligned} \frac{\lim_{h \rightarrow 0} h^{-1} \mathbb{P}(T^a \in [t, t+h] \mid T^a \geq t)}{\lim_{h \rightarrow 0} h^{-1} \mathbb{P}(T^0 \in [t, t+h] \mid T^0 \geq t)} &= \mathbb{E}[f_1(t, U_1, a) \mid T^a \geq t] \\ &= \int f_1(t, U_1, a) \frac{\exp(-\Lambda^a(t, U_1))}{\int \exp(-\Lambda^a(t, U_1)) dF_{U_1}} dF_{U_1}, \end{aligned}$$

where $\Lambda^a(t, u_1) = \int_0^t \lambda_0(s) f_1(s, u_1, a) ds$.

The MCHR thus equals $\mathbb{E}[f_1(t, U_1, a) \mid T^a \geq t]$, which is smaller than $\mathbb{E}[f_1(t, U_1, a)]$ as more weight is placed on lower values of $f_1(t, u_1, a)$ that correspond to higher $\mathbb{P}(T^a \geq t \mid U_1 = u_1)$. Besides the selection of frailty factors, the selection of individual modifiers can also lead to selection bias of the estimated hazard ratio. In contrast to $\mathbb{E}[f_0(t, U_0)]$ in the previous section, $\mathbb{E}[f_1(t, U_1, a) \mid T^a \geq t]$ decreases over time irrespective of whether the exposure is beneficial or harming on average. For a hypothetical setting without frailty but with effect heterogeneity, the CHR at t is thus systematically underestimated when using the MCHR, so the exposure seems more ‘beneficial’ than it is. Such a difference has only been explained by the presence of frailty (Hernán, 2010; Stensrud et al., 2017). For binary exposures and SCMs that further restrict $f_1(t, u_1, a) = u_1^a$, by Lemma 1 (as $\lambda_i^1 = U_{1i} \lambda_0(t)$),

$$\mathbb{E}[U_1 \mid T^1 \geq t] = -\frac{\mathcal{L}'_{U_1}(\int_0^t \lambda_0(s) ds)}{\mathcal{L}_{U_1}(\int_0^t \lambda_0(s) ds)}.$$

Let $\lambda_0 = \frac{t^2}{20}$, $U_1 \sim \Gamma(\frac{c}{\theta_1}, \frac{\theta_1}{c})$, $U_1 \sim \text{IG}(c, \frac{c^3}{\theta_1})$ or $U_1 \sim \text{CPoi}(3\frac{c^2}{\theta_1}, \frac{1}{2}, \frac{2\theta_1}{3c})$ respectively such that $\mathbb{E}[U_1] = c$ and $\text{var}(U_1) = \theta_1$. By applying Lemma 1 for $a = 1$, we can derive $\mathbb{E}[U_1 \mid T^1 \geq t]$, which by Corollary 2 (conditional hazard is monotone increasing) equal the MCHRs, and are presented in Table 2. Additionally, we derived $\mathbb{E}[U_1 \mid T^1 \geq t]$ for a setting where the multiplicative hazard effect modifier U_1 equals $\mu_1 (< 1$, for individuals that benefit) with probability p_1 , $\mu_2 (> 1$, for individuals that are harmed) with probability p_2 or 1 (for individuals that are not affected). We define this distribution as the Benefit-Harm-Neutral, BHN(p_1, μ_1, p_2, μ_2), distribution.

Table 2: Conditional expectation of the individual effect modifier U_1 when the CHR equals c for different modifier distributions such that $\mathbb{E}[U_1] = c$ and $\text{var}(U_0) = \theta_1$ (in absence of frailty).

	$U_1 \sim$			
	$\Gamma(\frac{c}{\theta_1}, \frac{\theta_1}{c})$	$\text{IG}(c, \frac{c^3}{\theta_1})$	$\text{CPoi}(3\frac{c^2}{\theta_1}, \frac{1}{2}, \frac{2\theta_1}{3c})$	BHN(p_1, μ_1, p_2, μ_2)
$\mathbb{E}[U_1 \mid T^1 \geq t]$	$\frac{60c^2}{\theta_1 t^3 + 60c}$	$\frac{c\sqrt{30c}}{\sqrt{t^3\theta_1 + 30c}}$	$c \left(\frac{\theta_1 t^3}{90c} + 1 \right)^{-\frac{3}{2}}$	$\frac{p_1 \mu_1 + p_2 \mu_2 e^{-\frac{t^3(\mu_2 - \mu_1)}{60}} + (1 - p_1 - p_2) e^{-\frac{t^3(1 - \mu_1)}{60}}}{p_1 + p_2 e^{-\frac{t^3(\mu_2 - \mu_1)}{60}} + (1 - p_1 - p_2) e^{-\frac{t^3(1 - \mu_1)}{60}}}$

For $\mathbb{E}[U_1] \in \{\frac{1}{3}, 3\}$, and $\theta_1 \in \{0.5, 1, 2\}$ the evolution of the conditional expectation is shown in Figure 3 for all four effect-modifier distributions. For the BHN distribution, when $\mathbb{E}[U_1]$ equals 3 and $\frac{1}{3}$, we fix

$p_1 = 0.05$, $\mu_1 = 0.5$ and $p_1 = 0.9$, $\mu_1 = 0.1$ respectively. Expressions for p_2 and μ_2 such that $\mathbb{E}[U_1] = \mu$ and $\text{var}(U_1) = \theta_1$ can be found in Appendix B.4. When the exposure is in expectation harming ($\mathbb{E}[U_1] = 3$), for all

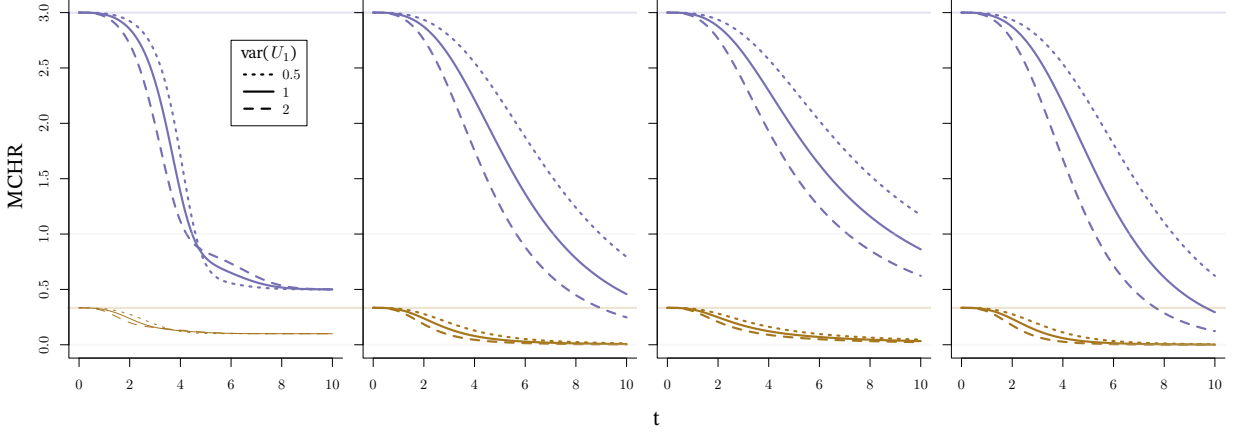


Fig. 3: MCHR over time when $\lambda_i^a(t) = \frac{t^2}{20}(U_{1i})^a$, when U_1 follows a BHN, gamma, inverse Gaussian or compound Poisson distribution (from left to right) with expectation 3 (blue) or $\frac{1}{3}$ (brown) and variance 0.5 (dotted), 1 (solid) or 2 (dashed) respectively.

settings considered there is a point in time that the MCHR drops below 1. For the continuous distributions, the MCHR won't stop decreasing. The decreases for the gamma and compound Poisson settings are very similar, while for the inverse Gaussian setting, this goes a bit slower. For the discrete setting, the marginal causal hazard converges to μ_1 of 0.5 and 0.1, respectively. Again, as in the previous subsection, the higher the variability of the latent variable, the faster the MCHR deviates from the CHR. Only for the discrete effect modifier, the lines cross for the different variances for $\mathbb{E}[U_1 = 3]$, but this is the result of different fractions of individuals that are not affected by the exposure (as the mean and variance are coupled).

4.3 Causal effect heterogeneity in the presence of frailty

In the general case where effect heterogeneity and frailty are present, both principles affect the value of the MCHR. By Theorem 2, the ratio evolves as $\frac{\mathbb{E}[f_0(t, U_0)f_1(t, U_1, a) | T^a \geq t]}{\mathbb{E}[f_0(t, U_0) | T^0 \geq t]}$. The numerator depends on the joint distribution of U_0 and U_1 . For illustration, we again consider a binary exposure and let

$$f_\lambda(t, U_{0i}, U_{1i}, a) = U_{0i}(U_{1i})^a \lambda_0(t) f_1(t, a),$$

such that the MCHR equals $\frac{\mathbb{E}[U_0 U_1 | T^1 \geq t]}{\mathbb{E}[U_0 | T^0 \geq t]} f_1(1, t)$ and, by Lemma 1, can be derived from the Laplace transforms of $U_0 U_1$ and U_0 respectively.

4.3.1 Independent U_0 and U_1

In the case of independence, the Laplace transform of the product equals $\mathbb{E}[\mathcal{L}_{U_0}(cU_1)]$, which generally does not adopt a tractable form. The case with a discrete effect modifier, introduced in Section 4.2, forms an exception. If $U_1 \sim \text{BHN}(p_1, \mu_1, p_2, \mu_2)$, then

$$\mathcal{L}_{U_0 U_1}(c) = p_1 \mathcal{L}_{U_0}(\mu_1 c) + p_2 \mathcal{L}_{U_0}(\mu_2 c) + (1 - p_1 - p_2) \mathcal{L}_{U_0}(c). \quad (15)$$

For the running example where $f_1(t, a) = 1$, $\lambda_0 = \frac{t^2}{20}$, $U_0 \sim \Gamma(\theta_0^{-1}, \theta_0)$, $U_0 \sim \text{IG}(1, \theta_0^{-1})$ or $U_0 \sim \text{CPois}(3\theta_0^{-1}, \frac{1}{2}, \frac{2}{3}\theta_0)$ for $\theta_0 \in \{0.5, 1, 2\}$, the expressions for $\mathbb{E}[U_0 U_1 \mid T^1 \geq t]$ are presented in Table 3 (where $p_3 = 1 - p_1 + p_2$ and $\mu_3 = 1$). As the $\mathbb{E}[U_0 \mid T^0 \geq t]$ are independent of the U_1 distribution these expectations are the same as presented in Table 1.

Table 3: Conditional expectation $\mathbb{E}[U_0 U_1 \mid T^1 \geq t]$ and its limiting forms when U_1 follows a $\text{BHN}(p_1, \mu_1, p_2, \mu_2)$ distribution) for different unit-expectations frailty distributions with $\text{var}(U_0) = \theta_0$ while $U_1 \perp U_0$. For comparison $\mathbb{E}[U_0 \mid T^0 \geq t]$, presented before in Table 1, is also presented

$U_0 \sim$	$\mathbb{E}[U_1 U_0 \mid T^1 \geq t]$	$\mathbb{E}[U_0 \mid T^0 \geq t]$
$\Gamma(\theta_0^{-1}, \theta_0)$	$\frac{\sum_{i=1}^3 p_i \mu_i \left(1 + \frac{\theta_0 t^3}{60} \mu_i\right)^{-(1+\theta_0^{-1})}}{\sum_{i=1}^3 p_i \left(1 + \frac{\theta_0 t^3}{60} \mu_i\right)^{-\theta_0^{-1}}}$ $= (\theta_0 \frac{t^3}{60})^{-1} + o(t^{-3})$	$\frac{60}{60 + t^3 \theta_0}$
$\text{IG}(1, \theta_0^{-1})$	$\frac{\sum_{i=1}^3 p_i \mu_i \left(2\theta_0 \frac{t^3}{60} \mu_i\right)^{-\frac{1}{2}} \exp\left(\theta_0^{-1} \left(1 - \sqrt{1 + \theta_0 2 \frac{t^3}{60} \mu_i}\right)\right)}{\sum_{i=1}^3 p_i \exp\left(\theta_0^{-1} \left(1 - \sqrt{1 + \theta_0 2 \frac{t^3}{60} \mu_i}\right)\right)}$ $= \sqrt{\mu_1} \sqrt{\frac{30}{t^3 \theta_0}} + o\left(t^{-\frac{3}{2}}\right)$	$\sqrt{\frac{30}{30 + t^3 \theta_0}}$
$\text{CPoi}\left(3\theta_0^{-1}, \frac{1}{2}, \frac{2}{3}\theta_0\right)$	$\frac{\sum_{i=1}^3 p_i \mu_i \left(\frac{3}{3 + 2\theta_0 \mu_i \frac{t^3}{60}}\right)^{\frac{3}{2}} \exp\left(3\theta_0^{-1} \sqrt{\frac{3}{3 + 2\theta_0 \mu_i \frac{t^3}{60}} - 1}\right)}{\sum_{i=1}^3 p_i \exp\left(3\theta_0^{-1} \sqrt{\frac{3}{3 + 2\theta_0 \mu_i \frac{t^3}{60}} - 1}\right)}$ $= 90^{\frac{3}{2}} (\theta_0 t^3)^{-\frac{3}{2}} \sum_{i=1}^3 \frac{p_i}{\sqrt{\mu_i}} + o\left(t^{-\frac{9}{2}}\right)$	$90^{\frac{3}{2}} (90 + t^3 \theta_0)^{-\frac{3}{2}}$

The MCHR and its limit can be derived from the expressions in Table 3 by applying Theorem 2 (conditional hazard is monotone increasing). Interestingly, for gamma frailty, this limit remains 1. For the inverse Gaussian frailty, the effect heterogeneity drastically change the limit from $\sqrt{\mathbb{E}[U_1]}$ to $\sqrt{\mu_1}$, which is always less than 1. Finally, for compound Poisson frailty the limit changes from $\sqrt{\mathbb{E}[U_1]}^{-1}$ to $\frac{p_1}{\sqrt{\mu_1}} + \frac{p_2}{\sqrt{\mu_2}} + (1 - p_1 - p_2)$. The evolution of $\frac{\mathbb{E}[U_0 U_1 \mid T^1 \geq t]}{\mathbb{E}[U_0 \mid T^0 \geq t]}$ over time is visualized in Figure 4 for $U_1 \sim \text{BHN}(0.05, 0.5, 0.82, 3.5)$, such that $\mathbb{E}[U_1] = 3$ and $\text{var}(U_1) = 1$, and for $U_1 \sim \text{BHN}(0.9, 0.1, 0.03, 6.0)$, such that $\mathbb{E}[U_1] = \frac{1}{3}$ and $\text{var}(U_1) = 1$.

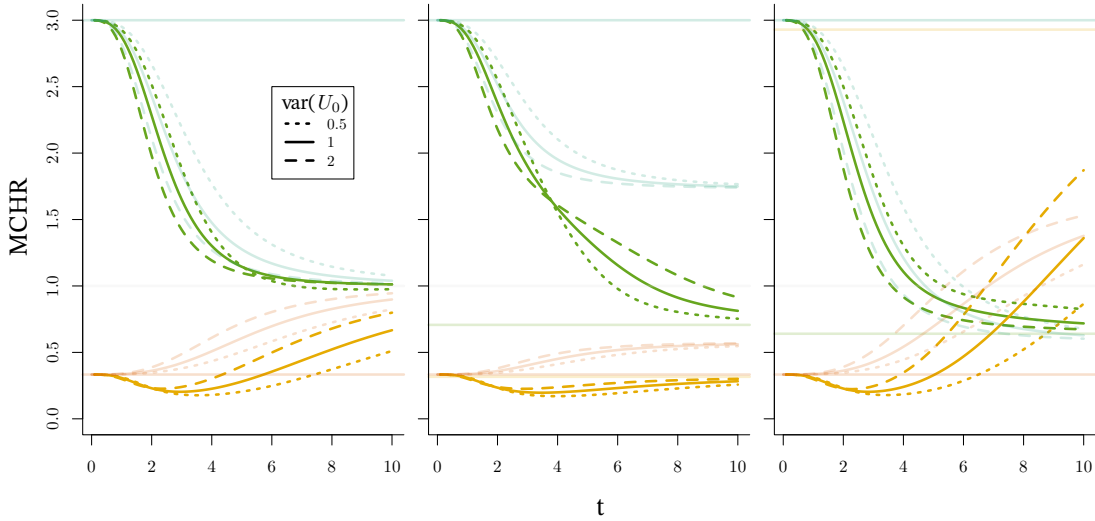


Fig. 4: MCHR over time when $\lambda_i^a(t) = U_{0i}(U_{1i})^a \frac{t^2}{20}$ for a unit-variance BHN distributed U_1 with $\mathbb{E}[U_1] = 3$ (opaque green) and $\mathbb{E}[U_1] = \frac{1}{3}$ (opaque orange), when U_0 follows a gamma (left), inverse Gaussian (middle) or compound Poisson (right) distribution with variance 0.5 (dotted), 1 (solid) or 2 (dashed) respectively. For comparison, the lines presented in Figure 2 are represented by transparent lines.

In the case the CHR is larger than 1, the selection of less susceptible individuals (frailty) that are harmed less (effect modifier) in the exposed world, both cause the MCHR to be smaller than the CHR. The MCHR decreases faster in the presence of effect heterogeneity. This explains the observation by Stensrud et al. (2017), “*Interestingly, the magnitude of frailty bias is larger when a heterogeneous treatment effect is included*”, for a simulation with frailty and random individual hazard ratios such that $\mathbb{E}[\lambda_i^1(t)] = 1.81 > 1$. For the gamma and compound Poisson frailty examples this effect is relatively small as $\mathbb{E}[U_1 U_0 | T^1 \geq t]$ is quite similar to $\mathbb{E}[U_0 | T^1 \geq t]$ as presented in Table 1 (for the presented p_1, μ_1, p_2 and μ_2). However, for inverse Gaussian frailty, the MCHR deviates much more from the CHR in the presence of effect heterogeneity. In Figure 5, the evolution of the MCHR is presented for a longer timescale, and the limits become apparent. If the CHR is smaller than 1, then the selection of less susceptible individuals (frailty) in the unexposed world and the selection of individuals that benefit more (effect modifier) in the exposed world have opposite effects on the MCHR. For this case of discrete effect modifiers, the MCHR first decreases by selecting individuals with more beneficial modifiers and later increases (above the CHR) when the frailty selection effect prevails. For the examples presented, the fraction $p_1 = 0.9$ of the population with $\mu_1 = 0.1$ are expected to survive so that over time the MCHR will resemble the MCHR in the absence of effect heterogeneity for this subpopulation (with the CHR equal to 0.1). The limit for gamma frailty is still one, so the MCHR deviates less from the CHR due to the two opposed selection effects. The bias is strongly reduced for the inverse Gaussian frailty as the limit $\sqrt{0.1}$ is close to the actual CHR. Finally, for the compound Poisson frailty, the MCHR with effect heterogeneity crosses the MCHR in the absence of effect heterogeneity as the frailty bias is larger for a CHR of 0.1 compared to one of $\frac{1}{3}$. In summary, the bias for the CHR can further increase in the presence of effect heterogeneity, stressing the issues regarding the causal interpretation of OHRs (assuming no confounding). However, for beneficial exposures, the frailty bias can reduce in the presence of effect heterogeneity (e.g., Inverse Gaussian frailty), illustrating that there might be settings where the MCHR is close to the CHR.

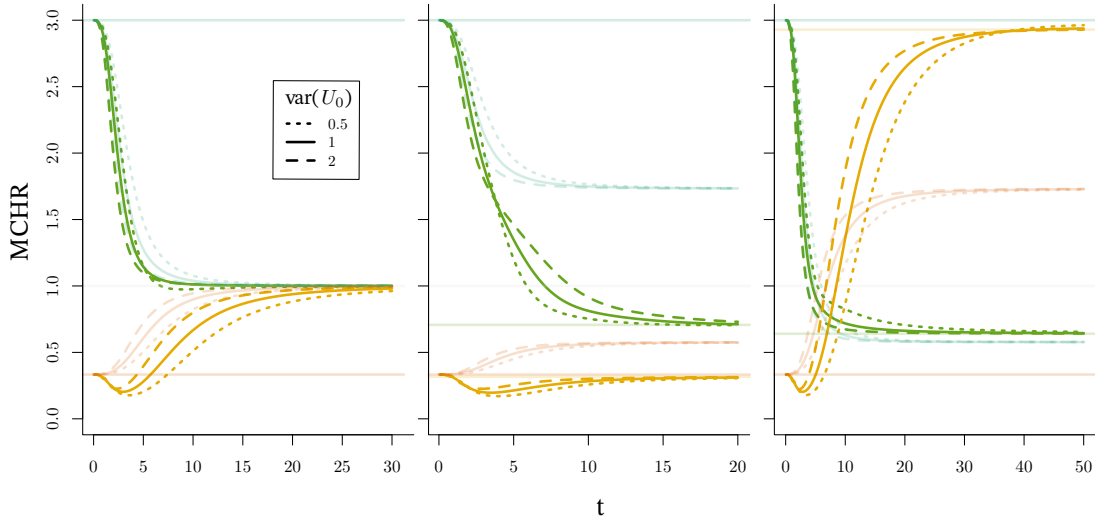


Fig. 5: MCHR over time when $\lambda_i^a(t) = U_{0i}(U_{1i})^a \frac{t^2}{20}$ for a unit-variance BHN distributed U_1 with $\mathbb{E}[U_1] = 3$ (opaque green) and $\mathbb{E}[U_1] = \frac{1}{3}$ (opaque orange), when U_0 follows a gamma (left), inverse Gaussian (middle) or compound Poisson (right) distribution with variance 0.5 (dotted), 1 (solid) or 2 (dashed) respectively. For comparison, the lines presented in Figure 2 as well as the limits of the MCHRs are represented by transparent lines.

4.3.2 Dependent U_0 and U_1

In case the multiplicative effect of the exposure on the hazard of susceptible individuals is expected to be higher or lower than for less susceptible individuals, the distribution of U_0U_1 will be less or more variable than when the latent variables are independent. Every bivariate joint distribution function can be written using the marginal distribution functions and a copula C (Sklar, 1959). As such,

$$F_{(U_0, U_1)}(u_0, u_1) = C(F_{U_0}(u_0), F_{U_1}(u_1))$$

and the Kendall's τ correlation coefficient of U_0 and U_1 can be written as a function of the Copula C (Nelsen, 2006). To study how the dependence can affect the MCHR for the setting presented in Figure 4, we use a Gaussian copula

$$C(x, y) = \Phi_{2, \rho}(\Phi^{-1}(x), \Phi^{-1}(y)),$$

where Φ and $\Phi_{2, \rho}$ are the standard normal and bivariate normal with correlation ρ , cumulative distribution functions, respectively. For $\rho \in \{-1, \sin(-\frac{\pi}{4}), 0, \sin(\frac{\pi}{4}), 1\}$ (such that $\tau \in \{-1, -0.5, 0, 0.5, 1\}$) and $\text{var}(U_0) = 1$, $\mathbb{E}[U_0U_1 | T^1 \geq t]$ is derived empirically from simulations and are presented in Figure 6. All programming codes used for this work can be found online at <https://github.com/RAJP93/CHR>. The results were very similar when using a Frank, Clayton or Gumbel copula instead of the Gaussian copula. For reference, the evolution of $\mathbb{E}[U_0 | T^0 \geq t]$ over time is also presented in Figure 6. The corresponding MCHRs are presented in Figure 7.

Note that for $\rho = 0$, we recover the independent setting already shown in Figure 4 that can be used for comparison. First of all, it is important to recall that when U_0 and U_1 are dependent the CHR equals $\mathbb{E}[U_1] + \text{cov}(U_0, U_1)$ as discussed in Section 3. For CHRs greater than 1, it becomes clear that the selection

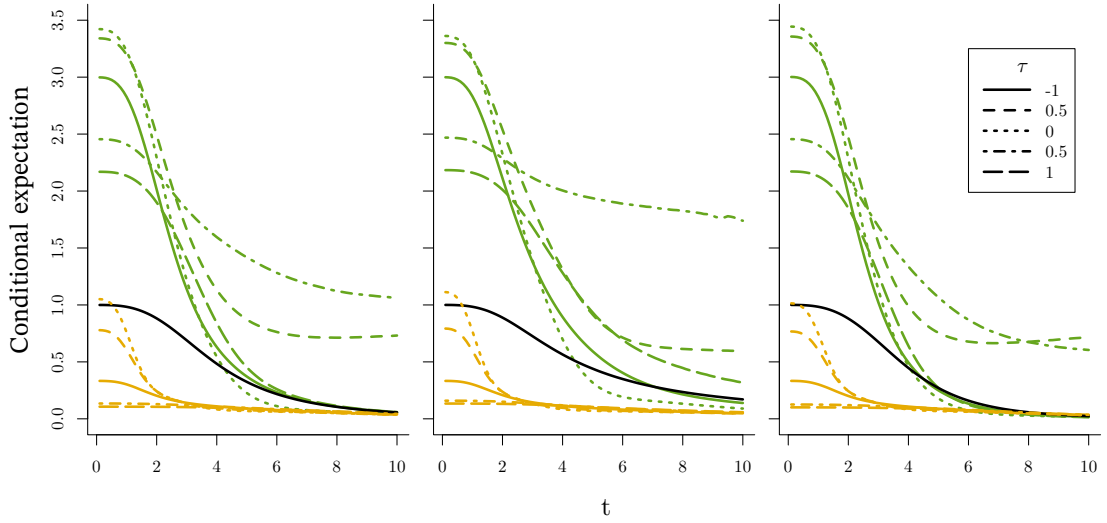


Fig. 6: $\mathbb{E}[U_0 U_1 \mid T^1 \geq t]$ over time for $\lambda_i^a(t) = U_{0i}(U_{1i})^a \frac{t^2}{20}$, for a unit-variance BHN distributed U_1 with $\mathbb{E}[U_1] = 3$ (green) or $\mathbb{E}[U_1] = \frac{1}{3}$ (orange), U_0 follows a gamma (left), inverse Gaussian (middle) or compound Poisson (right) distribution and where the joint distribution of U_0 and U_1 follows from a Gaussian copula with varying Kendall's τ correlation coefficient (see legend). Furthermore, the evolution of $\mathbb{E}[U_0 \mid T^0 \geq t]$ is presented (black).

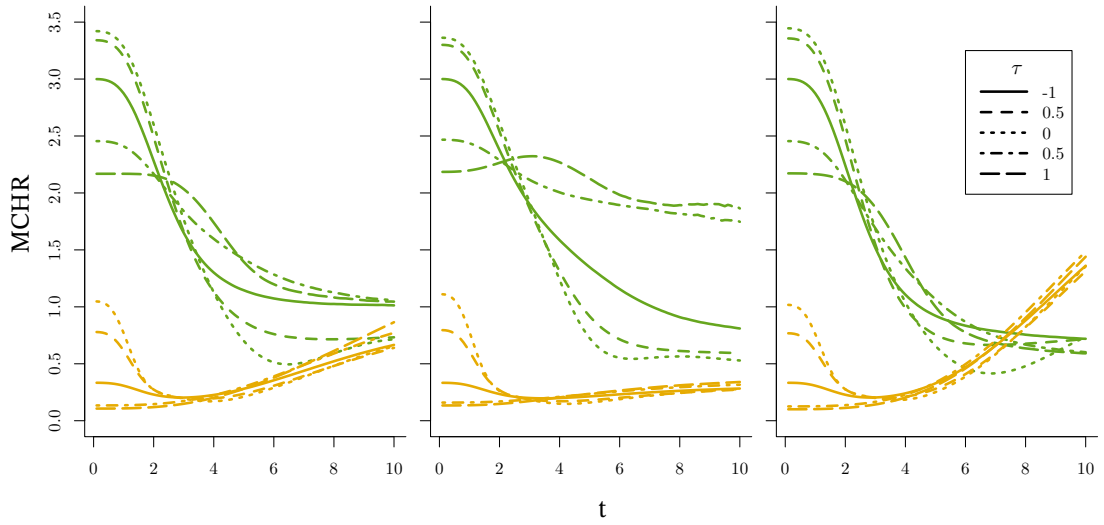


Fig. 7: MCHR over time for $\lambda_i^a(t) = U_{0i}(U_{1i})^a \frac{t^2}{20}$, for a unit-variance BHN distributed U_1 with $\mathbb{E}[U_1] = 3$ (green) or $\mathbb{E}[U_1] = \frac{1}{3}$ (orange), U_0 follows a gamma (left), inverse Gaussian (middle) or compound Poisson (right) distribution and where the joint distribution of U_0 and U_1 follows from a Gaussian copula with varying Kendall's τ correlation coefficient (see legend).

effect is more serious for cases with a high (positive) correlation between U_0 and U_1 . The stronger selection

effect is due to the higher variability of U_0U_1 . For CHRs less than 1, this trend is only true at short timescales, after which the frailty selection effect takes over since for this example a large fraction of the individuals, $p_1 = 0.9$, the effect is the same ($U_1 = 0.1$). When we use a continuous gamma distributed U_1 instead, the frailty selection effect is less apparent, as shown in Figure 8. So far, for CHRs larger than 1, we have observed

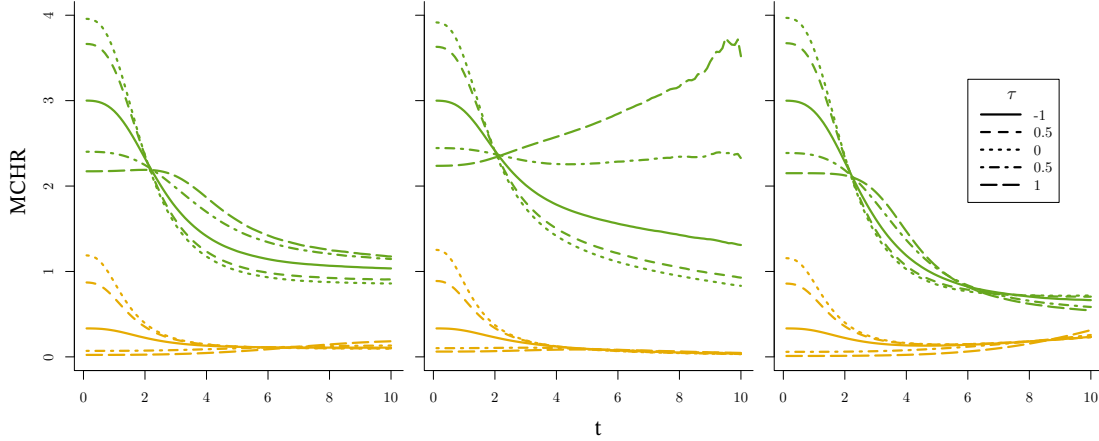


Fig. 8: MCHR over time for $\lambda_i^a(t) = U_{0i}(U_{1i})^a \frac{t^2}{20}$, for a unit-variance gamma distributed U_1 with $\mathbb{E}[U_1] = 3$ (green) or $\mathbb{E}[U_1] = \frac{1}{3}$ (orange), U_0 follows a gamma (left), inverse Gaussian (middle) or compound Poisson (right) distribution and where the joint distribution of U_0 and U_1 follows from a Gaussian copula with varying Kendall's τ correlation coefficient (see legend).

a monotonic MCHR. However, in the case of strong dependence between U_0 and U_1 ($\tau = -1$, and $\tau = 1$ for inverse Gaussian frailty) $\mathbb{E}[U_0 | T^0 \geq t]$ decreases faster than $\mathbb{E}[U_0U_1 | T^1 \geq t]$ resulting in a non-monotonic trend for the MCHR. For a Gamma distributed U_1 , in the case of inverse Gaussian distributed U_0 with $\tau = 1$, the MCHR even equals a monotonic increasing function over time as shown in Figure 8.

In this section, we have applied Theorem 1 to several examples to illustrate the deviation of the MCHR from the CHR. In summary, even when the CHR is constant, an OHR from an RCT equal to x (at time t) can occur for different CHR values when the (U_0, U_1) distribution is unknown as summarized in Table 4.

Table 4: Assuming no confounding, an OHR (at time t) equal to x can occur for all values of a constant CHR as a result of selection of the frailty (U_0) or modifier factor (U_1) which might be dependent.

		Cause	Presented examples
$x > 1$	$\text{CHR} > x$	Frailty or modifier selection	inverse Gaussian frailty - $\tau = 1$ (Figures 7, 8) compound Poisson frailty
	$1 < \text{CHR} < x$	Dependence U_0 and U_1	
	$\text{CHR} < 1$	Frailty selection	
$x < 1$	$\text{CHR} > 1$	Frailty or modifier selection	gamma distributed modifier (Figure 8)
	$x < \text{CHR} < 1$	Modifier selection	
	$\text{CHR} < x$	Frailty selection	

5 Implications for the Cox model

We have demonstrated that in the presence of frailty and effect heterogeneity, even when the CHR is constant, the MCHR varies over time. Then, the proportional hazards assumption will not hold for an OHR from an RCT (that is in the absence of informative censoring equal to the MCHR as discussed at the start of Section 4). Despite the many options to deal with non-proportional hazards (see, e.g. Therneau and Grambsch (2000, Section 6.5) or Hess (1994); Bennett (1983); Wei and Schaubel (2008)), in the majority of epidemiological time-to-event studies, the traditional Cox's proportional hazard model (that is thus misspecified) is fitted. The logarithm of the Cox estimate can be interpreted as the logarithm of the OHR marginalized over the observed death times (Schemper et al., 2009), i.e. $\mathbb{E}[\log(\text{OHR}(T)) \mid C = 0]$ for censoring indicator C . The logarithm of the Cox estimate obtained from an RCT thus equals a time-weighted average of the logarithm of the OHR. In the case of non-proportional hazards, even for uninformative censoring, the estimate is well-known to be affected by the censoring distribution. It differs from the average log hazard ratio $\mathbb{E}[\log(\text{OHR}(T))]$ (Schemper et al., 2009; Xu and O'Quigley, 2000; Boyd et al., 2012). Therefore, the bias of the Cox estimate, when the estimand is the CHR, will depend on the joint distribution of (U_0, U_1) as well as the censoring distribution. In most cases considered in Section 4, the deviation of the OHR from the CHR increased over time. For uninformative censoring, the probability of censoring increases over time, so the Cox estimate is closer to the OHR at short times. In Figure 9, this is demonstrated for the gamma-frailty case (Figure 4, $\text{var}(U_0) = 1$) by presenting empirically obtained $\mathbb{E}[\log(\text{OHR}(T)) \mid C = 0]$ (with 1,000,000 replications) based on a varying follow-up time and loss to follow-up modelled with an exponential censoring-time distribution with different parameters. The built-in selection bias of the OHR (assuming no confounding) emphasizes the

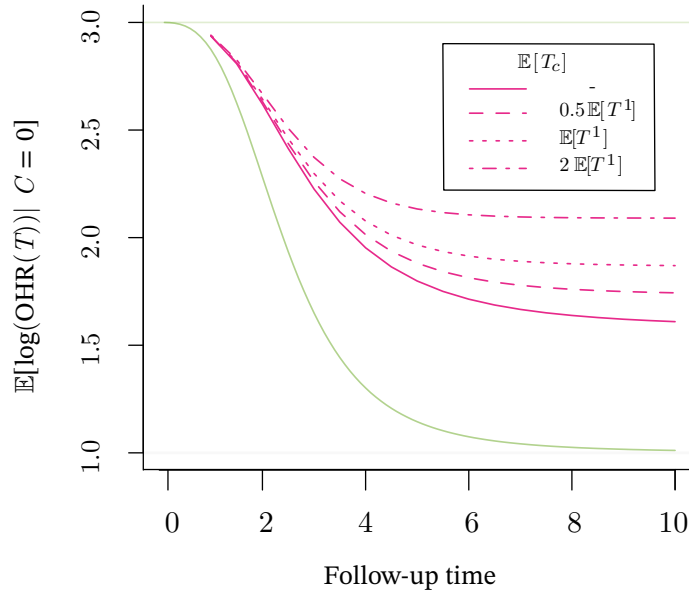


Fig. 9: Empirically obtained $\exp(\mathbb{E}[\log(\text{OHR}(T)) \mid C = 0])$ for increasing time-to follow up (solid pink), and for cases with an additional exponentially distributed censoring time (T_C , dashed pink), when $\lambda_i^a(t) = U_{0i}(U_{1i})^a \frac{t^2}{20}$, $U_1 \sim \text{BHN}(0.05, 0.5, 0.82, 3.5)$ and $U_0 \sim \Gamma(1, 1)$. The MCHR is also presented (green).

importance of testing the proportional hazard assumption. Serious bias will result in a time-varying OHR, so that violation of the proportional hazard assumption can be verified when fitting a Cox model. However, when the actual CHR would be time-varying, the OHR can be approximately constant when the selection effect and the change in CHR roughly cancels out (see, e.g. Stensrud et al. (2018)). The data cannot be used to distinguish the latter case from the case where there is no heterogeneity and, thus, no selection effect. Similarly, as already mentioned at the end of Section 3, when the OHR would vary over time, we can never conclude whether this is the result of a time-varying causal effect or due to selection. However, the proportional hazard assumption would be violated in this case, and a standard Cox model is inappropriate.

6 Discussion and concluding remarks

In this paper, we have formalized how heterogeneity leads to deviation of the MCHR (see Equation (9)) from the CHR of interest (see Definition 1) due to the selection of both the individual frailty factor (U_0) and the individual effect modifier (U_1). This work generalizes frailty examples presented in the literature (Hernán, 2010; Aalen et al., 2015; Stensrud et al., 2017), by considering the possibility of multiplicative effect (on the hazard) heterogeneity that also results in non-exchangeability of exposed and unexposed individuals over time. As a result of the individual effect modifier (U_1), the individuals that survive in the exposed groups are expected to benefit more (or suffer less) from the exposure. At the same time $U_0 | T^1 \geq t$ will have a different distribution than $U_0 | T^0 \geq t$. When the CHR is larger than 1 and $U_0 \perp U_1$, the selection effects act in the same direction. On the other hand, when the CHR is smaller than 1 and $U_0 \perp U_1$, the selection effects can act in opposite directions so that the MCHR might be closer to the CHR than in the case without effect heterogeneity (see Figure 4).

For data from an RCT, in the absence of informative censoring, the OHR equals the studied MCHR so that all results directly relate to the OHR. For observational data, the OHR does not equal the MCHR due to confounding. However, when all confounders \mathbf{L} are observed, i.e. $T^a \perp A | \mathbf{L}$, one can study the conditional (on \mathbf{L}) OHR that in turn is equal to the conditional MCHR. The presented theorems are valid while conditioning on \mathbf{L} .

The intuition explained by Hernán (2010) suggests that the MCHR underestimates the effect size, while the sign of the logarithms of the MCHR and the CHR are equal. However, we have shown that in the presence of effect heterogeneity, an MCHR equal to x can occur both under $\text{CHR} > 1$ as well as $\text{CHR} < 1$ as summarized in Table 4. Therefore, OHRs from RCTs are not guaranteed to present a lower bound for the causal effect without making untestable assumptions on the (U_0, U_1) distribution. We have derived how the MCHR will evolve due to the selection of frailty and effect modifiers in Theorem 1. However, in practice, only the evolution of the OHR can be found (assuming sufficient data is available). Even after assuming absence of confounding (e.g. in case of a RCT) the CHR is non-identifiable without making (untestable) assumptions on the (U_0, U_1) distribution as discussed at the end of Section 3.

We can thus not distinguish between a time-varying CHR without selection of U_0 and U_1 or a constant CHR with selection, see e.g. Stensrud and Hernán (2020). However, adjusting for other risk factors can lower the remaining variability of U_0 and U_1 so that the bias is reduced. Even for an RCT, it may thus help to focus on adjusted hazard ratios despite the absence of confounding. Nevertheless, adjusting for other risk factors will require more data and modelling decisions. We want to remark that although additive hazard models (when well-specified) do not suffer from the frailty selection as shown by Aalen et al. (2015), these models will suffer from latent modifier selection in the presence of effect heterogeneity ($\mathbb{E}[U_1 | T^1 \geq t] > \mathbb{E}[U_1]$) as demonstrated in our companion paper Post et al. (2022).

We hope that the discussed effect heterogeneity and formalization of the built-in selection bias of the OHR (in case of an RCT) show the need to use more appropriate estimands. As suggested by others, contrasts of the survival probabilities, the median, or the restricted mean survival time respectively of potential outcomes, are appropriate measures to quantify causal effects on time-to-event outcomes (Hernán, 2010; Bartlett et al., 2020; Stensrud et al., 2018; Young et al., 2020).

References

- Aalen OO, Cook RJ, Røysland K (2015) Does Cox analysis of a randomized survival study yield a causal treatment effect? *Lifetime Data Anal* 21(4):579–593
- Balan TA, Putter H (2020) A tutorial on frailty models. *Statistical Methods in Medical Research* 29(11):3424–3454
- Bartlett JW, Morris TP, Stensrud MJ, Daniel RM, Vansteelandt SK, Burman CF (2020) The hazards of period specific and weighted hazard ratios. *Statistics in Biopharmaceutical Research* 12(4):518–519
- Bennett S (1983) Analysis of survival data by the proportional odds model. *Statistics in Medicine* 2(2):273–277
- Bongers S, Forré P, Peters J, Mooij JM (2021) Foundations of structural causal models with cycles and latent variables. *The Annals of Statistics* 49(5):2885 – 2915
- Boyd AP, Kittelson JM, Gillen DL (2012) Estimation of treatment effect under non-proportional hazards and conditionally independent censoring. *Statistics in Medicine* 31(28):3504–3515
- Cox DR (1972) Regression models and life-tables. *Journal of the Royal Statistical Society Series B* 34(2):187–220
- Daniel R, Zhang J, Farewell D (2021) Making apples from oranges: Comparing noncollapsible effect estimators and their standard errors after adjustment for different covariate sets. *Biometrical Journal* 63(3):528–557
- De Neve J, Gerds TA (2020) On the interpretation of the hazard ratio in Cox regression. *Biometrical Journal* 62(3):742–750
- Didelez V, Stensrud MJ (2021) On the logic of collapsibility for causal effect measures. *Biometrical Journal*
- Hernán MA (2010) The hazards of hazard ratios. *Epidemiology* 21(1):13–15
- Hernán MA, Robins JM (2020) *Causal Inference: What If*. Boca Raton: Chapman & Hall/CRC
- Hernán MA, Hernández-Díaz S, Robins JM (2004) A structural approach to selection bias. *Epidemiology* 15(5):615–625
- Hernán MA, Cole SR, Margolick J, Cohen M, Robins JM (2005) Structural accelerated failure time models for survival analysis in studies with time-varying treatments. *Pharmacoepidemiology and Drug Safety* 14(7):477–491
- Hess KR (1994) Assessing time-by-covariate interactions in proportional hazards regression models using cubic spline functions. *Statistics in Medicine* 13(10):1045–1062
- Howe CJ, Cole SR, Lau B, Napravnik S, Eron JJ (2016) Selection bias due to loss to follow up in cohort studies. *Epidemiology* 27(1):91–97
- Martinussen T, Vansteelandt S (2013) On collapsibility and confounding bias in Cox and Aalen regression models. *Lifetime Data Analysis* 19(3):279–296
- Martinussen T, Vansteelandt S, Andersen P (2020) Subtleties in the interpretation of hazard contrasts. *Lifetime Data Analysis* 26(4):833–855
- Nelsen RB (2006) *An Introduction to Copulas*, 2nd edn. Springer
- Neyman J (1990) On the Application of Probability Theory to Agricultural Experiments. *Essay on Principles*. Section 9. *Statistical Science* 5(4):465–472

- Pearl J (2009) Causality: Models, reasoning, and inference, 2nd edn. Cambridge University Press, Cambridge
- Peters J, Janzing D, Schölkopf B (2018) Elements of causal inference: foundations and learning algorithms. The MIT Press, Cambridge, Massachusetts
- Post RAJ, van den Heuvel ER, Putter H (2022) Bias of the additive hazard model in the presence of causal effect heterogeneity
- author (2013) Single World Intervention Graphs (SWIGs): A Unification of the Counterfactual and Graphical Approaches to Causality. Tech. Rep. 128, University of Washington
- Rubin DB (1974) Estimating causal effects of treatments in randomized and nonrandomized studies. Journal of Educational Psychology 66(5):688–701
- Schemper M, Wakounig S, Heinze G (2009) The estimation of average hazard ratios by weighted cox regression. Statistics in Medicine 28(19):2473–2489
- Sjölander A, Dahlqvist E, Zetterqvist J (2016) A note on the noncollapsibility of rate differences and rate ratios. Epidemiology 27(3):356–359
- Sklar A (1959) Fonctions de répartition à n dimensions et leurs marges. Publications de l’Institut de statistique de l’Université de Paris 8:229–231
- Stensrud MJ, Hernán MA (2020) Why test for proportional hazards? JAMA 323(14):1401–1402
- Stensrud MJ, Valberg M, Røysland K, Aalen OO (2017) Exploring selection bias by causal frailty models: The magnitude matters. Epidemiology 28(3):379–386
- Stensrud MJ, Aalen JM, Aalen OO, Valberg M (2018) Limitations of hazard ratios in clinical trials. European Heart Journal 40(17):1378–1383
- Therneau TM, Grambsch PM (2000) Modeling Survival Data: Extending the Cox Model, 1st edn. Springer
- Wei G, Schaabel DE (2008) Estimating cumulative treatment effects in the presence of nonproportional hazards. Biometrics 64(3):724–732
- Xu R, O’Quigley J (2000) Estimating average regression effect under non-proportional hazards. Biostatistics 1(4):423–439
- Young JG, Stensrud MJ, Tchetgen Tchetgen EJ, Hernán MA (2020) A causal framework for classical statistical estimands in failure-time settings with competing events. Stat Med 39(8):1199–1236

A Proofs

A.1 Proof of Theorem 1

Proof

$$\begin{aligned}
 \frac{\mathbb{E}[\lambda_i^a(t)]}{\mathbb{E}[\lambda_i^0(t)]} &= \frac{\mathbb{E}[f_0(t, U_{0i})f_1(a, U_{1i}, t)]}{\mathbb{E}[f_0(t, U_{0i})]} \\
 &= \frac{\int \lim_{h \rightarrow 0} h^{-1} \mathbb{P}(T^a \in [t, t+h] \mid T^a \geq t, U_0, U_1) dF_{U_0, U_1}}{\int \lim_{h \rightarrow 0} h^{-1} \mathbb{P}(T^0 \in [t, t+h] \mid T^0 \geq t, U_0) dF_{U_0}} \\
 &= \frac{\int \lim_{h \rightarrow 0} h^{-1} \mathbb{P}(T^a \in [t, t+h] \mid T^a \geq t, U_0, U_1, A = a) dF_{U_0, U_1}}{\int \lim_{h \rightarrow 0} h^{-1} \mathbb{P}(T^0 \in [t, t+h] \mid T^0 \geq t, U_0, A = 0) dF_{U_0}} \\
 &= \frac{\int \lim_{h \rightarrow 0} h^{-1} \mathbb{P}(T \in [t, t+h] \mid T \geq t, U_0, U_1, A = a) dF_{U_0, U_1}}{\int \lim_{h \rightarrow 0} h^{-1} \mathbb{P}(T \in [t, t+h] \mid T \geq t, U_0, A = 0) dF_{U_0}}
 \end{aligned}$$

A.2 Proof of Theorem 2

Proof By the law of total probability,

$$\frac{\lim_{h \rightarrow 0} h^{-1} \mathbb{P}(T^a \in [t, t+h] \mid T^a \geq t)}{\lim_{h \rightarrow 0} h^{-1} \mathbb{P}(T^0 \in [t, t+h] \mid T^0 \geq t)} = \frac{\lim_{h \rightarrow 0} \int h^{-1} \mathbb{P}(T^a \in [t, t+h] \mid T^a \geq t, U_0, U_1) dF_{U_0, U_1 \mid T^a \geq t}}{\lim_{h \rightarrow 0} \int h^{-1} \mathbb{P}(T^0 \in [t, t+h] \mid T^0 \geq t, U_0) dF_{U_0 \mid T^0 \geq t}}$$

First we focus on the integrand,

$$\begin{aligned} & h^{-1} \mathbb{P}(T^a \in [t, t+h] \mid T^a \geq t, U_0, U_1) \\ &= h^{-1} \frac{\mathbb{P}(T^a \geq t \mid U_0, U_1) - \mathbb{P}(T^a \geq t+h \mid U_0, U_1)}{\mathbb{P}(T^a \geq t \mid U_0, U_1)} \\ &= h^{-1} \left(1 - \frac{\mathbb{P}(T^a \geq t+h \mid U_0, U_1)}{\mathbb{P}(T^a \geq t \mid U_0, U_1)} \right) \\ &= h^{-1} \left(1 - \frac{\exp\left(-\int_0^{t+h} f_0(s, U_0) f_1(s, U_1, a) ds\right)}{\exp\left(-\int_0^t f_0(s, U_0) f_1(s, U_1, a) ds\right)} \right) \\ &= h^{-1} \left(1 - \exp\left(-\int_t^{t+h} f_0(s, U_0) f_1(s, U_1, a) ds\right) \right) \end{aligned}$$

For monotonic (increasing or decreasing) conditional hazard functions if $h_2 < h_1$, then

$$h_1^{-1} \left(1 - \exp\left(-\int_t^{t+h_1} f_0(s, U_0) f_1(s, U_1, a) ds\right) \right) \leq h_2^{-1} \left(1 - \exp\left(-\int_t^{t+h_2} f_0(s, U_0) f_1(s, U_1, a) ds\right) \right)$$

or

$$h_1^{-1} \left(1 - \exp\left(-\int_t^{t+h_1} f_0(s, U_0) f_1(s, U_1, a) ds\right) \right) \geq h_2^{-1} \left(1 - \exp\left(-\int_t^{t+h_2} f_0(s, U_0) f_1(s, U_1, a) ds\right) \right)$$

as the average integrated conditional hazard over the interval increases (or decreases). Then, the limit and integral can be interchanged by directly applying the monotone convergence theorem.

For non-monotone conditional hazard functions, let $h \leq \tilde{h}$, and note

$$h^{-1} \mathbb{P}(T^a \in [t, t+h] \mid T^a \geq t, U_0, U_1) \leq h^{-1} (1 - \exp(-h f_0(t^*, U_0) f_1(t^*, U_1, a)))$$

where

$$\max_{s \in (t, t+\tilde{h})} f_0(s, U_0) f_1(s, U_1, a) = f_0(t^*, U_0) f_1(t^*, U_1, a).$$

Using the power series definition of the exponential function,

$$\begin{aligned} & h^{-1} \mathbb{P}(T^a \in [t, t+h] \mid T^a \geq t, U_0, U_1) \\ & \leq h^{-1} \left(1 - \frac{1}{\sum_{k=0}^{\infty} h^k (f_0(t^*, U_0) f_1(t^*, U_1, a))^k \frac{1}{k!}} \right) \\ & = h^{-1} \frac{\sum_{k=1}^{\infty} h^k (f_0(t^*, U_0) f_1(t^*, U_1, a))^k \frac{1}{k!}}{\sum_{k=0}^{\infty} h^k (f_0(t^*, U_0) f_1(t^*, U_1, a))^k \frac{1}{k!}} \\ & = f_0(t^*, U_0) f_1(t^*, U_1, a) \frac{\sum_{k=1}^{\infty} h^{k-1} (f_0(t^*, U_0) f_1(t^*, U_1, a))^{k-1} \frac{1}{k!}}{\sum_{k=0}^{\infty} h^k (f_0(t^*, U_0) f_1(t^*, U_1, a))^k \frac{1}{k!}} \\ & = f_0(t^*, U_0) f_1(t^*, U_1, a) \frac{\sum_{k=0}^{\infty} h^k (f_0(t^*, U_0) f_1(t^*, U_1, a))^k \frac{1}{(k+1)!}}{\sum_{k=0}^{\infty} h^k (f_0(t^*, U_0) f_1(t^*, U_1, a))^k \frac{1}{k!}} \\ & < f_0(t^*, U_0) f_1(t^*, U_1, a). \end{aligned}$$

Furthermore, $\mathbb{E}[f_0(t^*, U_0)f_1(t^*, U_1, a) | T^a \geq t] < \infty$ when $\forall h \in (0, \tilde{h}) : \mathbb{E}[f_0(t+h, U_0)f_1(t+h, U_1, a) | T^a \geq t] < \infty$. Then we can change the order of the limit and integral by application of the dominated convergence theorem and conclude,

$$\frac{\lim_{h \rightarrow 0} h^{-1} \mathbb{P}(T^a \in [t, t+h] | T^a \geq t)}{\lim_{h \rightarrow 0} h^{-1} \mathbb{P}(T^0 \in [t, t+h] | T^0 \geq t)} = \frac{\mathbb{E}[f_0(t, U_0)f_1(t, U_1, a) | T^a \geq t]}{\mathbb{E}[f_0(t, U_0) | T^0 \geq t]}.$$

Applying Bayes rule, we obtain

$$\begin{aligned} & \mathbb{E}[f_0(t, U_0)f_1(t, U_1, a) | T_i^a \geq t] \\ &= \int f_0(t, U_0)f_1(t, U_1, a) dF_{(U_0, U_1) | T^a \geq t} \\ &= \int f_0(t, U_0)f_1(t, U_1, a) \frac{\mathbb{P}(T^a \geq t | U_0, U_1)}{\mathbb{P}(T^a \geq t)} dF_{(U_0, U_1)} \\ &= \int f_0(t, U_0)f_1(t, U_1, a) \frac{\exp(-\int_0^t f_0(s, U_0)f_1(s, U_1, a) ds)}{\int \exp(-\int_0^t f_0(s, U_0)f_1(s, U_1, a) ds) dF_{(U_0, U_1)}} dF_{(U_0, U_1)}. \end{aligned}$$

Furthermore,

$$\begin{aligned} & \mathbb{E}[f_0(t, U_0) | T^a \geq t] \\ &= \int f_0(t, U_0) dF_{U_0 | T_i^a \geq t} \\ &= \int f_0(t, U_0) \frac{\mathbb{P}(T^a \geq t | U_0)}{\mathbb{P}(T^a \geq t)} dF_{U_0} \\ &= \int f_0(t, U_0) \frac{\int \exp(-\int_0^t f_0(s, U_0)f_1(s, U_1, a) ds) dF_{U_1 | U_0}}{\int \exp(-\int_0^t f_0(s, U_0)f_1(s, U_1, a) ds) dF_{(U_0, U_1)}} dF_{U_0}, \end{aligned}$$

such that for $a = 0$,

$$\mathbb{E}[f_0(t, U_0) | T^0 \geq t] = \int f_0(t, U_0) \frac{\exp(-\int_0^t f_0(s, U_0) ds)}{\int \exp(-\int_0^t f_0(s, U_0) ds) dF_{U_0}} dF_{U_0}.$$

The ratio of both gives us the result.

A.3 Proof of Corollary 1

Proof By Theorem 2,

$$\frac{\lim_{h \rightarrow 0} h^{-1} \mathbb{P}(T^a \in [t, t+h] | T^a \geq t)}{\lim_{h \rightarrow 0} h^{-1} \mathbb{P}(T^0 \in [t, t+h] | T^0 \geq t)} = \frac{\mathbb{E}[f_0(t, U_0)f_1(t, U_1, a) | T^a \geq t]}{\mathbb{E}[f_0(t, U_0) | T^0 \geq t]}.$$

and equals

$$\int f_0(t, U_0)f_1(t, U_1, a) \frac{\exp(-\Lambda^a(t, U_0, U_1))}{\int \exp(-\Lambda^a(t, U_0, U_1)) dF_{(U_0, U_1)}} dF_{(U_0, U_1)} \left(\int f_0(t, U_0) \frac{\exp(-\Lambda^0(t, U_0))}{\int \exp(-\Lambda^0(t, U_0)) dF_{U_0}} dF_{U_0} \right)^{-1},$$

where $\Lambda^a(t, u_0, u_1) = \int_0^t f_0(s, u_0)f_1(s, u_1, a) ds$ and thus $\Lambda^0(t, u_0) = \int_0^t f_0(s, u_0) ds$. As U_1 is degenerate,

$$\begin{aligned} & \int f_0(t, U_0) \frac{\exp(-\int_0^t f_0(s, U_0)f_1(a, s) ds)}{\int \exp(-\int_0^t f_0(s, U_0)f_1(a, s) ds) dF_{U_0}} dF_{U_0} \left(\int f_0(t, U_0) \frac{\exp(-\int_0^t f_0(s, U_0) ds)}{\int \exp(-\int_0^t f_0(s, U_0) ds) dF_{U_0}} dF_{U_0} \right)^{-1} f_1(t, a) \\ &= \frac{\mathbb{E}[f_0(t, U_0) | T_i^a \geq t]}{\mathbb{E}[f_0(t, U_0) | T_i^0 \geq t]} f_1(t, a). \end{aligned}$$

A.4 Proof of Lemma 1

Proof By Bayes rule, the probability density $f_{U_0|T^a \geq t}$ equals

$$\begin{aligned} f_{U_0|T^a \geq t}(u_0) &= \frac{\mathbb{P}(T^a \geq t | U_0 = u_0)f(u_0)}{\int \mathbb{P}(T^a \geq t | U_0)dF_{U_0}} \\ &= \frac{\exp(-u_0 \int_0^t \lambda_0(s)f_1(a, s)ds)f_{U_0}(u_0)}{\int \exp(-U_0 \int_0^t \lambda_0(s)f_1(a, s)ds)dF_{U_0}}. \end{aligned}$$

Such that the Laplace transform of $U_0 | T^a \geq t$ can be written as

$$\begin{aligned} \mathcal{L}_{U_0|T^a \geq t}(c) &= \mathbb{E}[\exp(-U_0 c) | T^a \geq t] \\ &= \int \exp(-u_0 c) f_{U_0|T^a \geq t}(u_0) du_0 \\ &= \int \exp(-u_0 c) \frac{\exp(-u_0 \int_0^t \lambda_0(s)f_1(a, s)ds)f_{U_0}(u_0)}{\int \exp(-U_0 \int_0^t \lambda_0(s)f_1(a, s)ds)dF_{U_0}} dF_{U_0} \\ &= \int \frac{\exp(-u_0(c + \int_0^t \lambda_0(s)f_1(a, s)ds))f_{U_0}(u_0)}{\int \exp(-U_0 \int_0^t \lambda_0(s)f_1(a, s)ds)dF_{U_0}} dF_{U_0} \\ &= \frac{\mathbb{E} \left[\exp(-U_0(c + \int_0^t \lambda_0(s)f_1(a, s)ds)) \right]}{\mathbb{E} \left[\exp(-U_0 \int_0^t \lambda_0(s)f_1(a, s)ds) \right]} \\ &= \frac{\mathcal{L}_{U_0}(c + \int_0^t \lambda_0(s)f_1(a, s)ds)}{\mathcal{L}_{U_0}(\int_0^t \lambda_0(s)f_1(a, s)ds)}. \end{aligned}$$

Since for a random variable X , $\mathbb{E}[X] = -\mathcal{L}'_X(0)$,

$$\mathbb{E}[U_0 | T^a \geq t] = -\mathcal{L}'_{U_0|T^a \geq t}(0) = -\frac{\mathcal{L}'_{U_0}(\int_0^t \lambda_0(s)f_1(a, s)ds)}{\mathcal{L}_{U_0}(\int_0^t \lambda_0(s)f_1(a, s)ds)}.$$

A.5 Proof of Corollary 2

Proof By Theorem 2,

$$\frac{\lim_{h \rightarrow 0} h^{-1} \mathbb{P}(T^a \in [t, t+h] | T^a \geq t)}{\lim_{h \rightarrow 0} h^{-1} \mathbb{P}(T^0 \in [t, t+h] | T^0 \geq t)} = \frac{\mathbb{E}[f_0(t, U_0)f_1(t, U_1) | T^a \geq t]}{\mathbb{E}[f_0(t, U_0) | T^0 \geq t]}.$$

and equals

$$\int f_0(t, U_0)f_1(t, U_1, a) \frac{\exp(-\Lambda^a(t, U_0, U_1))}{\int \int \exp(-\Lambda^a(t, U_0, U_1))dF_{(U_0, U_1)}} dF_{(U_0, U_1)} \left(\int f_0(t, U_0) \frac{\exp(-\Lambda^0(t, U_0))}{\int \exp(-\Lambda^0(t, U_0))dF_{U_0}} dF_{U_0} \right)^{-1},$$

where $\Lambda^a(t, u_0, u_1) = \int_0^t f_0(s, u_0)f_1(s, u_1, a)ds$ and thus $\Lambda^0(t, u_0) = \int_0^t f_0(s, u_0)ds$. As now U_0 is degenerate,

$$\int f_1(t, U_1, a) \frac{\exp(-\Lambda^a(t, U_1))}{\int \exp(-\Lambda^a(t, U_1))dF_{U_1}} dF_{U_1} = \mathbb{E}[f_1(t, U_1, a) | T_i^a \geq t],$$

where $\Lambda^a(t, u_1) = \int_0^t \lambda_0(s)f_1(s, u_1, a)ds$.

B Laplace transforms

B.1 Gamma

If $X \sim \Gamma(k, \theta)$, then $\mathbb{E}[X] = k\theta$, $\text{var}[X] = k\theta^2$,

$$\mathcal{L}_X(c) = (1 + \theta c)^{-k},$$

$$\mathcal{L}'_X(c) = -\frac{\theta k}{\theta c + 1} \mathcal{L}_X(c),$$

and

$$\mathcal{L}''_X(c) = \frac{\theta^2 k(k+1)}{(\theta c + 1)^2} \mathcal{L}_X(c).$$

When $f_\lambda(t, U_{0i}, U_{1i}, a) = U_{0i} \lambda_0(t) f_1(t, a)$, by Lemma 1,

$$\mathbb{E}[U_0 | T^a \geq t] = \frac{\theta k}{\theta \Lambda^a(t) + 1}, \quad (16)$$

where $\Lambda^a(t) = \int_0^t \lambda_0(s) f_1(a, s) ds$. If $\mathbb{E}[U_0] = c$ and $\text{var}(U_0) = \theta$, then $k = \frac{c^2}{\theta_0}$, $\theta = \frac{\theta_0}{c}$ and as such

$$\mathbb{E}[U_0 | T^a \geq t] = \frac{c}{\frac{\theta_0}{c} \Lambda^a(t) + 1}. \quad (17)$$

In particular, when $k = \theta^{-1}$, then $\mathbb{E}[U_0] = 1$, $\text{var}(U_0) = \theta$ and

$$\mathbb{E}[U_0 | T^a \geq t] = (\theta \Lambda^a(t) + 1)^{-1}. \quad (18)$$

B.2 Inverse Gaussian

If $X \sim \text{IG}(\mu, \lambda)$, then $\mathbb{E}[X] = \mu$, $\text{var}[X] = \frac{\mu^3}{\lambda}$,

$$\mathcal{L}_X(c) = \exp\left(\frac{\lambda}{\mu} \left(1 - \sqrt{1 + \frac{2\mu^2 c}{\lambda}}\right)\right),$$

$$\mathcal{L}'_X(c) = -\frac{\mu}{\sqrt{\frac{2\mu^2 c}{\lambda} + 1}} \mathcal{L}_X(c),$$

and

$$\mathcal{L}''_X(c) = \left(\mu^2 \frac{\lambda}{\lambda + 2\mu^2 c} + \frac{\mu}{\lambda \left(\frac{2\mu^2 c}{\lambda} + 1\right)^{\frac{3}{2}}}\right) \mathcal{L}_X(c).$$

When $f_\lambda(t, U_{0i}, U_{1i}, a) = U_{0i} \lambda_0(t) f_1(t, a)$, by Lemma 1,

$$\mathbb{E}[U_0 | T^a \geq t] = \frac{\mu}{\sqrt{\frac{2\Lambda^a(t)\mu^2}{\lambda} + 1}}, \quad (19)$$

where $\Lambda^a(t) = \int_0^t \lambda_0(s) f_1(a, s) ds$. If $\text{var}(U_0) = \theta_0$, then $\lambda = \frac{\mu^3}{\theta_0}$ and as such

$$\mathbb{E}[U_0 | T^a \geq t] = \frac{\mu}{\sqrt{2\Lambda^a(t) \frac{\theta_0}{\mu} + 1}}. \quad (20)$$

In particular when $\mu = 1$ and $\lambda = \theta_0^{-1}$, then $\mathbb{E}[U_0] = 1$, $\text{var}(U_0) = \theta_0$ and

$$\mathbb{E}[U_0 | T^a \geq t] = (2\theta_0 \Lambda^a(t) + 1)^{-\frac{1}{2}}. \quad (21)$$

B.3 Compound Poisson

If $X \sim \text{CPois}(\rho, \eta, \nu)$, then $X = \sum_{i=1}^N Y_i$, where $N \sim \text{Poi}(\rho)$, and $Y \sim \Gamma(\eta, \nu)$, $\mathbb{E}[X] = \rho\eta\nu$, $\text{var}[X] = \rho\eta\nu^2 + \eta^2\nu^2\rho$,

$$\mathcal{L}_X(c) = \exp\left(\rho\left(\left(\frac{\nu^{-1}}{\nu^{-1}+c}\right)^\eta - 1\right)\right),$$

$$\mathcal{L}'_X(c) = -\rho\eta\nu\left(\frac{1}{c\nu+1}\right)^{\eta+1}\mathcal{L}_X(c),$$

and

$$\mathcal{L}''_X(c) = \eta\nu^2\rho\left(\frac{1}{c\nu+1}\right)^{\eta+2}\left(\eta\rho\left(\frac{1}{c\nu+1}\right)^\eta + \eta + 1\right)\mathcal{L}_X(c).$$

When $f_\lambda(t, U_{0i}, U_{1i}, a) = U_{0i}\lambda_0(t)f_1(t, a)$, by Lemma 1,

$$\mathbb{E}[U_0 | T^a \geq t] = \rho\eta\nu\left(\frac{1}{\Lambda^a(t)\nu+1}\right)^{\eta+1}, \quad (22)$$

where $\Lambda^a(t) = \int_0^t \lambda_0(s)f_1(a, s)ds$. Let $\mathbb{E}[U_0] = c$ and $\text{var}(U_0) = \theta_0$, then $\rho = \frac{c^2(1+\eta)}{\eta\theta_0}$, $\nu = \frac{\theta_0}{c(1+\eta)}$ and as such

$$\mathbb{E}[U_0 | T^a \geq t] = c\left(\frac{1}{\Lambda^a(t)\frac{\theta_0}{c(1+\eta)}+1}\right)^{\eta+1}. \quad (23)$$

In particular, when $\eta = \frac{1}{2}$, $\rho = 3\theta^{-1}$ and $\nu = \frac{2}{3}\theta$, then $\mathbb{E}[U_0] = 1$, $\text{var}(U_0) = \theta$ and

$$\mathbb{E}[U_0 | T^a \geq t] = (1 + \Lambda^a(t)\frac{2}{3}\theta)^{-\frac{3}{2}}. \quad (24)$$

B.4 Discrete

Let $\mathbb{P}(X = \mu_i) = p_i$ for $i > 0$, $i \leq k$,

$$\mathcal{L}_X(c) = \sum_{i=1}^n p_i \exp(-c\mu_i),$$

$$\mathcal{L}'_X(c) = \sum_{i=1}^n -\mu_i p_i \exp(-c\mu_i),$$

and

$$\mathcal{L}''_X(c) = \sum_{i=1}^n \mu_i^2 p_i \exp(-c\mu_i).$$

Furthermore, if $Y \sim F$, then

$$\mathcal{L}_{XY}(c) = \sum_{i=1}^n p_i \mathcal{L}_Y(c\mu_i),$$

$$\mathcal{L}'_{XY}(c) = \sum_{i=1}^n p_i \mu_i \mathcal{L}'_Y(c\mu_i),$$

and

$$\mathcal{L}''_{XY}(c) = \sum_{i=1}^n p_i \mu_i^2 \mathcal{L}''_Y(c\mu_i).$$

Let U_1 equal μ_1 , μ_2 or 1 with probability p_1 , p_2 and $1 - p_1 - p_2$ respectively. If

$$p_2 = \frac{(\mu - \mu_1 p_1 + p_1 - 1)^2}{\mu^2 - 2\mu - \mu_1^2 p_1 + 2\mu_1 p_1 - p_1 + \theta_1 + 1},$$

and

$$\mu_2 = \frac{\mu^2 - \mu - \mu_1^2 p_1 + \mu_1 p_1 + \theta_1}{\mu - \mu_1 p_1 + p_1 - 1},$$

such that $p_2 \in [0, 1]$ and $\mu_2 \geq 1$, then $\mathbb{E}[U_1] = \mu$ and $\text{var}(U_1) = \theta_1$. When, $f_\lambda(t, U_{0i}, U_{1i}, a) = \lambda_0(t)(U_{1i})^a f_1(t, a)$, by Lemma 1,

$$\mathbb{E}[U_1 | T^1 \geq t] = \frac{\mu_1 p_1 e^{-\Lambda^1(t)\mu_1} + \mu_2 p_2 e^{-\Lambda^1(t)\mu_2} + (1 - p_1 - p_2) e^{-\Lambda^1(t)}}{p_1 e^{-\Lambda^1(t)\mu_1} + p_2 e^{-\Lambda^1(t)\mu_2} + (1 - p_1 - p_2) e^{-\Lambda^1(t)}}, \quad (25)$$

where $\Lambda^1 = \int_0^t \lambda_0(s) f_1(1, s) ds$.

Furthermore, when $f_\lambda(t, U_{0i}, U_{1i}, a) = U_{0i} \lambda_0(t) (U_{1i})^a f_1(t, a)$, and U_0 and U_1 are independent, by Lemma 1,

$$\mathbb{E}[U_0 U_1 | T^1 \geq t] = \frac{p_1 \mu_1 \mathcal{L}'_{U_0}(\Lambda^1 \mu_1) + p_2 \mu_2 \mathcal{L}'_{U_0}(\Lambda^1 \mu_2) + (1 - p_1 - p_2) \mathcal{L}'_{U_0}(\Lambda^1)}{p_1 \mathcal{L}_{U_0}(\Lambda^1 \mu_1) + p_2 \mathcal{L}_{U_0}(\Lambda^1 \mu_2) + (1 - p_1 - p_2) \mathcal{L}_{U_0}(\Lambda^1)}. \quad (26)$$

C Survival curves examples

The survival curves of T^0 and T^1 for the examples presented in this paper can be expressed in terms of the Laplace transforms presented in the previous section as shown in Table 5, where $\Lambda_0(t) = \frac{t^3}{60}$. For the example where $U_0 \not\perp U_1$, the survival curve for T^1 is obtained empirically from simulation. For data from a RCT $T^a \stackrel{d}{=} T | A = a$.

Table 5: Survival curves for T^0 and T^1 for different $\lambda_i^a(t)$ where $\Lambda_0(t) = \frac{t^3}{60}$.

$\lambda_i^a(t)$	$S_{T^0}(t)$	$S_{T^1}(t)$
$U_{0i} \frac{t^2}{20} c^a$	$\mathcal{L}_{U_0}(\Lambda_0(t))$	$\mathcal{L}_{U_0}(c\Lambda_0(t))$
$\frac{t^2}{20} (U_{1i})^a$	$\exp(-\Lambda_0(t))$	$\mathcal{L}_{U_1}(\Lambda_0(t))$
$U_{0i} \frac{t^2}{20} (U_{1i})^a$	$\mathcal{L}_{U_0}(\Lambda_0(t))$	$\mathcal{L}_{U_0 U_1}(\Lambda_0(t))$

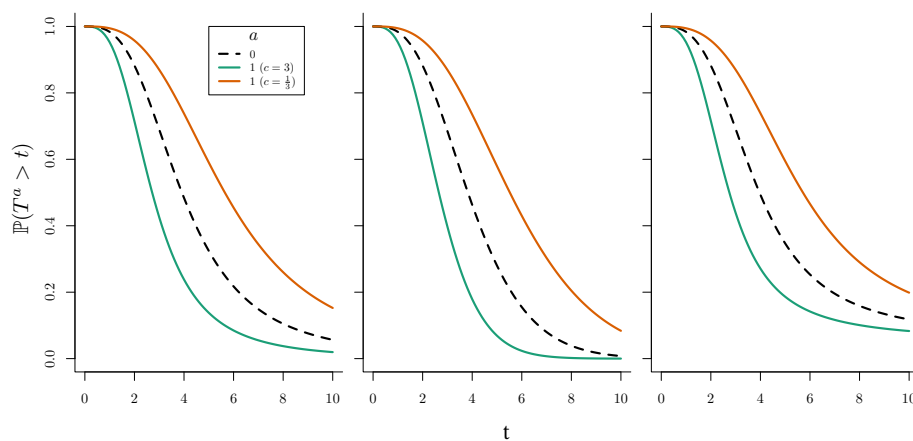


Fig. 10: Survival curves for T^0 (black), and T^1 (colored) when $\lambda_i^a(t) = U_{0i} \frac{t^2}{20} c^a$ for $c = 3$ (green) and $c = \frac{1}{3}$ (orange), when U_0 follows a gamma, inverse Gaussian or compound Poisson distribution (from left to right) with variance 1. The corresponding MCHR curves were presented in Figure 2.

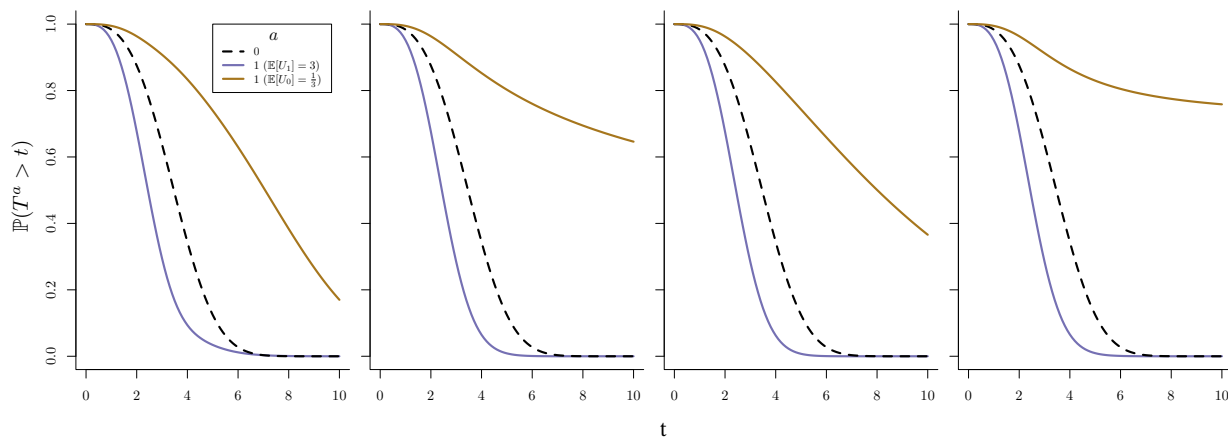


Fig. 11: Survival curves for T^0 (black), and T^1 (colored) when $\lambda_i^a(t) = U_{0i} \frac{t^2}{20} (U_{1i})^a$, when U_1 follows a BHN, gamma, inverse Gaussian or compound Poisson distribution (from left to right) with expectation 3 (blue) or $\frac{1}{3}$ (brown) and variance 1. The corresponding MCHR curves were presented in Figure 3.

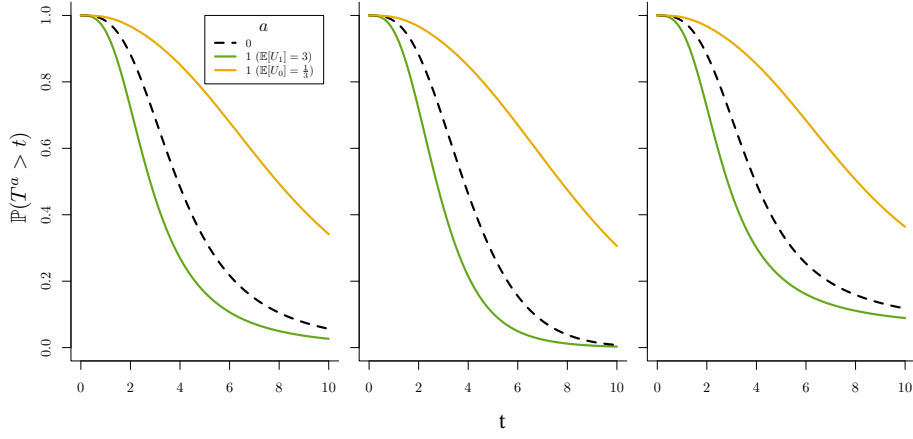


Fig. 12: Survival curves for T^0 (black), and T^1 (colored) when $\lambda^a(t)_i = U_{0i}(U_{1i})^a \frac{t^2}{20}$ for a unit-variance BHN distributed U_1 with $\mathbb{E}[U_1] = 3$ (green) and $\mathbb{E}[U_1] = \frac{1}{3}$ (orange), when U_0 follows a gamma, inverse Gaussian or compound Poisson distribution (from left to right) with variance 1. The corresponding MCHR curves were presented in Figure 4.

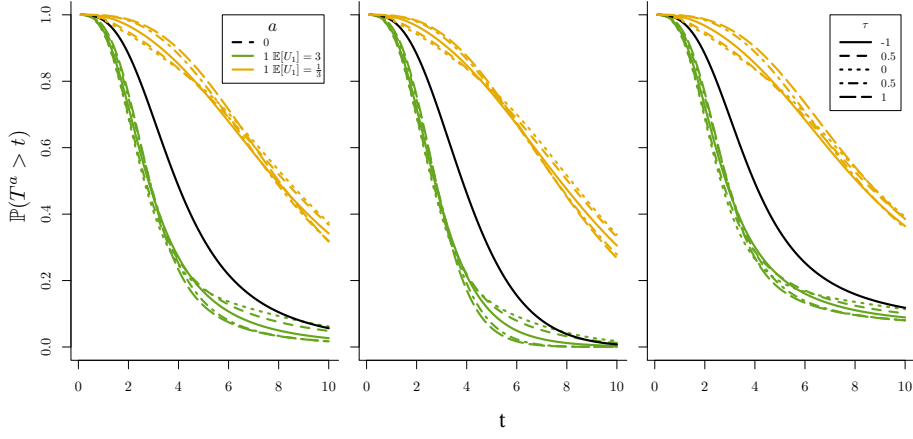


Fig. 13: Survival curves for T^0 (black), and T^1 (colored) when $\lambda_i^a(t) = U_{0i}(U_{1i})^a \frac{t^2}{20}$, for a unit-variance BHN distributed U_1 with $\mathbb{E}[U_1] = 3$ (green) or $\mathbb{E}[U_1] = \frac{1}{3}$ (orange), when U_0 follows a gamma, inverse Gaussian or compound Poisson distribution (from left to right) with variance 1 and where the joint distribution of U_0 and U_1 follows from a Gaussian copula with varying Kendall's τ . The corresponding MCHR curves were presented in Figure 7.

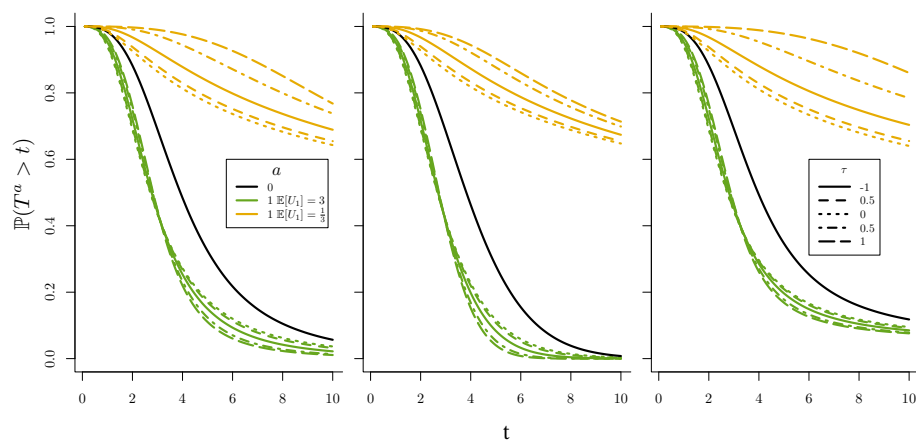


Fig. 14: Survival curves for T^0 (black), and T^1 (colored) when $\lambda_i^\alpha(t) = U_{0i}(U_{1i})^\alpha \frac{t^2}{20}$, for a unit-variance gamma distributed U_1 with $\mathbb{E}[U_1] = 3$ (green) or $\mathbb{E}[U_1] = \frac{1}{3}$ (orange), when U_0 follows a gamma, inverse Gaussian or compound Poisson distribution (from left to right) with variance 1, and where the joint distribution of U_0 and U_1 follows from a Gaussian copula with varying Kendall's τ . The corresponding MCHR curves were presented in Figure 8.